# Path-oriented synchronized transit scheduling using time-dependent data

Lee, Kelvin; Jiang, Yu ; Ceder, Avishai (Avi) ; Dauwels, Justin; Su, Rong ; Nielsen, Otto Anker

**DOI**
10.1016/j.trc.2021.103505

**Publication date**
2022

**Document Version**
Final published version

**Published in**
Transportation Research Part C: Emerging Technologies

Transportation Research Part C 136 (2022) 103505

Contents lists available at ScienceDirect

Transportation Research Part C

journal homepage: www.elsevier.com/locate/trc

# Path-oriented synchronized transit scheduling using time-dependent data

Kelvin Lee [a,b], Yu Jiang [c,*], Avishai (Avi) Ceder [d,e], Justin Dauwels [f], Rong Su [a], Otto Anker Nielsen [c]

[a] School of Electrical and Electronic Engineering, Nanyang Technological University, Singapore
[b] Energy Research Institute@ NTU, Interdisciplinary Graduate Programme, Nanyang Technological University, Singapore
[c] Transport DTU, Technical University of Denmark (DTU), Denmark
[d] Faculty of Civil and Environmental Engineering and the Transportation Research Institute, Technion-Israel Institute of Technology, Israel
[e] Key Laboratory of Transport, Beijing Jiaotong University (BJTU), PR China
[f] Department of Microelectronics, Faculty of Electrical Engineering, Mathematics, and Computer Science, Delft University of Technology (TU Delft), The Netherlands

ARTICLE INFO

*Keywords:*
Public transport
Schedule synchronization
Time-dependent data
Valid inequality

ABSTRACT

With the emergence of innovations associated with public transport (PT) services, such as Mobility-as-a-Service, demand responsive transit, and autonomous vehicles, the door-to-door PT journey is achievable via multiple transfers between and within different PT modes. As such, seamless transfers between different modes of public transportation become an increasingly important factor for the attractiveness of PT services. At the same time, recent developments in travel time prediction methodologies offer new, reliable data sources for the optimization of PT operations. This work, with the consideration of these two elements, develops a mixed integer linear programming model for the PT schedule synchronization problem. The novelty is threefold. First, a novel concept of path-oriented scheduling is proposed. The path transfer time is explicitly formulated and minimized to provide a seamless travel experience considering that the emerging multimodal mobility inevitably induces multiple transfers. Second, time-dependent travel time data is also utilized in the model, which allows us to harness new and more representative data sources for improving PT services. Third, in order to complement the increase in computational complexity as a result of the utilization of time-dependent travel time data, three novel valid inequalities (VIs) are derived. Numerical studies show that the use of time-dependent travel time data is beneficial in terms of reducing path transfer times, when compared to using the mean historical travel times. The numerical study also reveals a tradeoff between the maximum allowable path transfer time and trip time. Using simulation studies on three bus lines in Copenhagen, we demonstrate that the valid inequalities could reduce the computation time by 8.5% on average, where the maximum reduction of computation time could reach 54.0%. The proposed valid inequalities are benchmarked against two classes of valid inequalities in the literature. It is found that the proposed valid inequalities could outperform those in the literature. We also found that further improvement in computational performance can be attained by using a combination of the proposed valid inequalities.

* Corresponding author.
*E-mail addresses:* kelvin003@e.ntu.edu.sg (K. Lee), yujiang@dtu.dk (Y. Jiang), ceder@technion.ac.il (A. Ceder), j.h.g.dauwels@tudelft.nl (J. Dauwels), rsu@ntu.edu.sg (R. Su), oani@dtu.dk (O.A. Nielsen).

https://doi.org/10.1016/j.trc.2021.103505
Received 14 May 2021; Received in revised form 29 November 2021; Accepted 30 November 2021
Available online 17 January 2022

## 1. Introduction

Various innovations in the field of public transport (PT) are currently flourishing, such as Mobility-as-a-Service (MaaS), demand responsive transit (DRT), autonomous vehicles (AVs) for transit, and customized buses. PT operators strive to provide door-to-door PT services that approach a level of integration and convenience comparable to that of private cars, which is crucial in encouraging mode shift from private cars to transit service (Chakrabarti, 2017) and promoting sustainable urban mobility (Ceder, 2021). For captive transit riders, who depend on public transit services on a daily basis, the improvement of services will also help to improve social equity (Milan and Creutzig, 2017). A key attribute that contributes to the general quality of public transit is the quality of transfers (Ceder and Teh, 2010; Ceder, 2016). Multiple travel behavioral studies have concluded that passengers are often averse to transfers and tend to prefer direct connections (Hine and Scott, 2000; Beirão and Sarsfield Cabral, 2007). Interviewees often cite long waiting times, the risk of missing connecting buses at the interchanges and perceived inconvenience as the contributing factors to their attitude towards PT. These problems can be solved through careful planning and synchronization of PT schedules. In particular, Badia et al. (2017) and Guo and Wilson (2011) have found that by improving the transfer experience, PT can benefit significantly in terms of passengers' satisfaction and overall public transit ridership.

While there exists a vast literature on PT timetable synchronization, one aspect that is considerably lacking is the consideration of the passengers' overall travel experience. Most studies in the literature consider synchronization at each stop independent of each other by maximizing the aggregate number of synchronized services at each stop. Doing so, however, means that other important attributes that contribute to a passenger's overall experience, like waiting time at the origin and transfer stops, in-vehicle travel time and transfer time are not considered. This work, for the first time proposes the concept of path-oriented schedule synchronization, which considers the passengers' itineraries as a whole and jointly optimize the aforementioned attributes. In summary, the contributions of this work is threefold:

1. This study develops a mixed integer linear programming formulation for the PT schedule synchronization problem. The concept of path-oriented synchronization, which focuses on the complete trips, is incorporated in the formulation in order to improve the overall transfer experience.
2. The formulation takes as input the time-dependent travel time data to reflect the temporal variations of travel time throughout the planning horizon to improve synchronization of schedules.
3. Valid inequalities are devised based on domain knowledge and model properties to curb the increase in computational complexity which comes with the use of time-dependent travel time data.

The remainder of this paper is structured as follows: In Section 2, we review previous studies that are relevant to this work. Section 3 introduces assumptions and notations used throughout the paper and the formulation for the schedule synchronization problem is presented. The valid inequalities are derived in Section 4, whereas the numerical studies are presented in Section 5. Finally, Section 6 summarizes our findings and indicates future research directions.

## 2. Related works

In this section, we review the literature on two aspects that are related to our work, i.e. (1) PT schedule synchronization and (2) the use of time-dependent travel time in PT schedule synchronization. In the first part, we review the models and solution methods developed to solve the PT schedule synchronization problem. We also identify a major shortcoming that is common in these works and a gap that we attempt to address in this work. In the latter part of this section, we look into the use of time-dependent travel time data to solve optimization problems within the field of transportation and the benefits that come with their use.

### *2.1. PT schedule synchronization*

There are quite a few studies on PT scheduling and timetable synchronization problems. The state-of-the-art review can be found in Ibarra-Rojas et al. (2015) and Ceder (2016). Early approaches adopted quadratic programming to determine PT line departure times at an interchange station for minimizing the total transfer cost considering a given transfer demand (Klemt and Stemme, 1988; Bookbinder and Désilets, 1992; Wu et al., 2021). Wong et al. (2008) devised a binary decision variable to express the waiting time explicitly, given that all transfer passengers will board the first arriving connecting train. Instead of using waiting time at transfer stops to measure the schedule synchronization, some studies proposed the use of the number of simultaneous bus arrivals and formulated a mixed integer formulation to determine the departure times of buses (Ceder et al., 2001; Ceder and Tal, 2001). Ibarra-Rojas and Rios-Solis (2012) modeled the feasibility of synchronization as a binary decision variable, which equals one if the arrivals of two trips occur within the same time window. They proved that their problem is an NP-hard problem and employed a multi-start iterated local search algorithm to solve the model. The same decision variable was adopted in Ibarra-Rojas et al. (2015) and Fouilhoux et al. (2016). Other than optimizing schedule synchronization, Ceder et al. (2013) proposed considering even-headway and even-load simultaneously in determining bus timetables. A graphical heuristic approach was developed to solve the problem. Ye and Liu (2016) adopted an optimal control methodology for scheduling problems and considered energy consumption as their objective. Wu et al. (2016) incorporated a safety control margin into the scheduling problem to counteract stochasticity in the travel time. Recently, Abdolmaleki et al. (2020) modeled the scheduling optimization model as an optimization problem with congruence constraints and developed an efficient approximation algorithm.

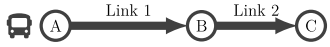


| Link no. | Time window | Travel time (min) |
|---|---|---|
| 1 | 08:01 a.m. - 08:10 a.m. | 5 |
| | 08:11 a.m. - 08:20 a.m. | 9 |
| 2 | 08:01 a.m. - 08:10 a.m. | 3 |
| | 08:11 a.m. - 08:20 a.m. | 6 |

**Fig. 1.** An illustrative example of time-dependent travel times.

Nonetheless, most existing studies, while focusing on minimizing the total transfer cost or maximizing the number of synchronizations at stops, do not consider the total transfer costs associated with each passenger. This is a crucial shortcoming common of these works because many ordinary PT trips (i.e., bus and metro) involve more than one transfer. Moreover, emerging innovations associated with PT services, such as AVs and MaaS, results in more transfers between and within travel modes when compared to the traditional PT journey. Thus, the transfer experience for each PT journey will not only affect passengers' travel costs but will also be part of the perceived attractiveness of PT and mobility services. Contrary to conventional wisdom, Badia et al. (2017) has found that increasing the number of transfer trips could also increase patronage using PT service by providing a transfer-friendly network. In such a network, when one or more transfers are inevitable, passengers will direct their attention to the accumulated experience throughout all the transfer points along the journey, rather than only the transfer experience at one station. Therefore, we identify this as a gap in the literature and attempt to address it by considering a path-based formulation for the PT synchronization problem. In this formulation, we shall take into account the passengers' path from their origins to destinations and the costs associated with all the transfers involved.

### *2.2. Use of time-dependent travel time data in solving transportation problems*

With the development of data collection technologies, such as smart cards, bluetooth, smartphone applications, and the development of prediction models, availability of time-dependent and short-term real-time demand (van Oort et al., 2015; Menon and Lee, 2017) and supply data (Yu et al., 2011; O'Sullivan et al., 2016; Zhou et al., 2017; Pang et al., 2019; Rahman et al., 2018; Petersen et al., 2019; Liu et al., 2020) has increased considerably. Various studies on the utilization of time-dependent demand data for scheduling PT services have been conducted (Niu and Zhou, 2013; Niu et al., 2015; Yue et al., 2017). On the contrary, the methodology for utilizing time-dependent supply data for PT scheduling is not well-established. Time-dependent travel time data has already been utilized to obtain promising results in the context of vehicle routing problems (Malandraki and Daskin, 1992), pathfinding problems (Hall, 1986), and vehicle scheduling problems (Ichoua et al., 2003). In the context of PT scheduling, to the best of our knowledge, Wang et al. (2017) is the only study that is more closely related to this paper. In Wang et al. (2017), the authors devised a model to minimize total passenger waiting time by scheduling metro service and demonstrated that the use of time-dependent data can significantly reduce the total passenger waiting time. Nevertheless, the paper did not consider passenger transfer time and schedule synchronization. This paper, therefore, aims to fill in these gaps by investigating the use of time-dependent travel time data in the PT schedule synchronization problem and quantify the benefit of doing so.

## 3. Formulation

### *3.1. Motivations for the use of time-dependent travel time data*

To demonstrate the effect of time-dependent travel time on transit schedules, we use an illustrative transit line as presented in Fig. 1. Each vehicle traverses stops A, B and C through two consecutive links. In this example, the time interval for which the time-dependent travel times remain valid is 10 min, and the travel time of each link depends on the time at which a vehicle enters the links. For instance, if a vehicle enters link 1 between 8:01 a.m. and 8:10 a.m., the travel time through the link is 5 min. The travel time becomes 9 min should the vehicle enter the link between 8:11 a.m. and 8:20 a.m. If a vehicle enters link 1 at 8:09 a.m., it shall arrive at stop B at 8:14 a.m., as the travel time remains at 5 min despite the fact that the vehicle will still be traversing link 1 between 8:11 a.m. and 8:20 a.m.

Consider two departures from station A, at 8:01 a.m. and 8:09 a.m. respectively, and a fixed dwell time of 1 min at each stop. The first bus arrives stop B at 8:06 a.m., and enters link 2 at 8:07 a.m. after the one-minute dwell time. As the bus enters link 2 at 8:07 a.m., the travel time through link 2 shall be 3 min, which means the bus shall arrive at stop C at 8:10 a.m. Similarly, the second bus departs stop A at 8:09 a.m., and arrives at stop C at 8:21 a.m. (5 min through link 1, dwell time of 1 min and 6 min through link 2).

In comparison to the first bus, the arrival time difference between the two buses is 11 min, despite the 8 min difference in the departure time from stop A. Hence, it is important that time-dependent travel time data is used in PT schedule synchronization because a small disparity in the departure and arrival times of a single transit line can induce a chain effect which can potentially cause long transfer times and passenger dissatisfaction.

In this study, as we have noted previously, the time-dependent travel time of each link is determined by the time a vehicle enters a link. Generally speaking, with higher resolution travel time data, the smaller the interval for which the travel time is assumed to be constant and the more accurate the estimated travel time will be. However, this comes at the cost of additional investments in the data collection systems and computational infrastructures.

### 3.2. Assumptions

The following assumptions are made throughout the paper:

A1. The services to be synchronized are schedule-based services. The services do not follow a fixed frequency, but they must conform to the allowable headway range that is predetermined. The headway range shall be published and communicated to the public such that passengers can make informed transit decisions with the information given.

A2. Time-dependent travel time data are given. This is a reasonable assumption because the data is readily available to bus operators. In Copenhagen, for example, the PT agency, Movia can provide the data. However, the data is not fully utilized to optimize bus services yet. The methodology for estimating these data is beyond the scope of this study.

A3. All passengers are able to board the first arriving vehicle of the desired transit line, and the capacity constraint and congestion effect are not considered. This is a common assumption in PT scheduling literature (Ceder et al., 2001; Wong et al., 2008; Ibarra-Rojas and Rios-Solis, 2012).

A4. Dwell time is independent of passenger flow. A lower bound of the dwell time is set to ensure that there is enough time for travelers to board and alight. If the resultant dwell time is higher than the lower bound of the dwell time, it can be interpreted, to some extent, as a holding strategy at the stop.

A5. The travel demand and departure time are known and deterministic as is commonly assumed in the literature (Nuzzolo et al., 2001; Nuzzolo and Crisalli, 2004; Poon et al., 2004; Hamdouch et al., 2014). In practice, the travel demand and departure time can be estimated form smart card data or a mobile phone app. Thus, it is reasonable to assume that the data is available to a PT operator.

### 3.3. Problem description

#### 3.3.1. Notations

Consider a general PT network, where the set of transit lines and the set of stops are denoted as $R$ and $S$ respectively. The transit lines could be of different PT modes, such as bus, metro, or an autonomous vehicle(AV)-based PT service. A transit line $r \in R$ represents a unidirectional service traversing a sequence of stations $S_r = \left(s_r^{(1)}, \ldots, s_r^{(|S_r|)}\right)$ sequentially with buses indexed by $k \in K_r = \{1, \ldots, |K_r|\}$. All possible transfers in the network are represented by a set of 3-tuples $\Psi = \left\{ (r, r', s) | r, r' \in R, s \in S_r \cap S_{r'} \neq \varnothing \right\}$, where $r$ and $r'$ are two transit lines that serve a common station $s$. The planning horizon is discretized into $|T|$ time intervals, such that each $\tau \in T$ represents the time interval $[\tau\vartheta, (\tau+1)\vartheta)$ where $\vartheta$ is the duration of each time interval. In this study, we assume that the travel time of each link remains constant throughout each 15-minutes time interval. The travel time between station $s_r^{(i)}$ and station $s_r^{(i+1)}$ within time interval $[\tau\vartheta, (\tau+1)\vartheta)$ is denoted by $t^{\tau}_{rs^{(i)}}$. Note that the index for transit line $r$ is dropped from the $s_r^{(i)}$ in $t^{\tau}_{rs^{(i)}}$ when the same $r$ is used.

On the demand side, passengers are grouped based on their departure time, origin, destination and path choices. Each passenger group $g \in G$ has $Q_g$ passengers who intend to depart from their origin stop at time $F_g$, and travel via the same path towards the same destination. The path for each group is associated with two attributes, a sequence of stops $S_g = \left(s_g^{(i)}\right)_{i=0}^{|S_g|-1}$ and a sequence of PT lines $R_g = \left(r_g^{(i)}\right)_{i=1}^{|S_g|-1}$. The transfers associated with each passenger group are represented by a sequence of 3-tuples, $\Psi_g = \left(\left(r_g^{(i)}, r_g^{(i+1)}, s_g^{(i)}\right)\right)_{i=1}^{|S_g|-2}$. For passengers using a direct path, we have $\Psi_g = \varnothing$. We define another sequence of 3-tuples, $\Phi_g = \left(\left(r_g^{(i)}, s_g^{(i-1)}, s_g^{(i)}\right)\right)_{i=1}^{|S_g|-1}$, as the sequence of in-vehicle segments associated with the itinerary of passenger group $g$.

In the remaining of this paper, all input parameters in the model are denoted by capital letters, while all decision variables are denoted by lower case letters.

#### 3.3.2. Formulation

Based on the preceding assumptions, the proposed optimization model aims to determine the optimal values for the decision variables presented in Table 1, where we provide a non-exhaustive list of notations used in the formulation. Other auxiliary variables will be introduced when they are first used in the formulation below.

Before we define the objective function for the model, we shall look into the anatomy of a passengers' itinerary and define some variables. Three passenger itineraries are plotted on time axes in Fig. 2. The time at which the passengers arrive at their origin stops are given by $F_g$ (marked by yellow diamonds), whereas the time spent at the origin stop waiting for the next bus is denoted by $w_g$ (marked by $A$). The passengers take the next bus until they arrive at the first transfer stop (marked by $B$), at which they transfer to the platform of a different route (marked by $C$). The transfer time between these platforms are denoted by $W_{rr's}$. The passengers then wait at the platform for the connecting route, for the next bus (marked by $D$), and the process repeats itself until the passengers arrive at their destinations. We define the time between the arrival of the passengers at a transfer stop $a^k_{rs}$ and the

**Table 1**
Notations used in the optimization formulation.

| Notation | Definition |
|---|---|
| Sets and indices | |
| $R$ | Set of routes |
| $S$ | Set of stations |
| $K$ | Set of bus indices |
| $T$ | Set of time windows |
| $\Psi$ | Set of transfers |
| $\Phi$ | Set of in-vehicle segments |
| $G$ | Set of passenger groups |
| Parameters | |
| $\underline{H}_r, \overline{H}_r$ | Minimum and maximum allowable headway for transit line $r$ |
| $\underline{U}_{rs}, \overline{U}_{rs}$ | Minimum and maximum allowable dwell time for transit line $r$ at station $s$ |
| $\vartheta$ | Size of time intervals for which time-dependent travel time remains constant |
| $t^{\tau}_{rs^{(i)}}$ | Travel time from station $s_r^{(i)}$ to station $s_r^{(i+1)}$ on transit line $r$ within time window $\tau$ |
| $T_{rss'}$ | Mean travel time from station $s$ to $s'$ on route $r$ |
| $\overline{P}_g$ | Maximum allowable path transfer time for group $g$ |
| $Q_g$ | Number of passengers in passenger group $g$ |
| $F_g$ | Arrival time of passenger group $g$ at their origin station $s_g^{(0)}$ |
| $\left[\underline{A}_g, \overline{A}_g\right]$ | Time interval within which arrival of passenger group $g$ at their destination station $s_g^{(\lvert S_g\rvert-1)}$ is considered on time |
| $W_{rr's}$ | Walk time between platforms of route $r$ and $r'$ at station $s$ |
| $\overline{D}$ | Planning horizon, i.e. the time by which all bus have to depart from their origin |
| $C_w, C_v, C_p, C_e, C_l$ | Value of time weights for the different time-related attributes |
| Decision variables | |
| $a^k_{rs}$ | Arrival time of the $k$th vehicle of transit line $r$ at station $s$ |
| $u^k_{rs}$ | Dwell time of the $k$th vehicle of transit line $r$ at station $s$ |
| $d^k_{rs}$ | Departure time of the $k$th vehicle of transit line $r$ from station $s$ |
| $t^{kk'}_{rr's}$ | Transfer time incurred when passengers transfer from the $k$th vehicle of line $r$ to the $k'$th vehicle of line $r'$ at station $s$ |
| $\varphi^{k\tau}_{rs}\in\{0,1\}$ | Denotes whether the $k$th vehicle of transit line $r$ departs station $s$ within time window $\tau$ |
| $\Delta^{kk'}_{rr's}\in\{0,1\}$ | Denotes whether the transfer from the $k$th vehicle of line $r$ to the $k'$th vehicle of line $r'$ is feasible (i.e. the $k'$th vehicle of transit line $r'$ departs $s$ no earlier than the arrival of passengers traveling on the $k$th vehicle of transit line $r$ at the platform for transit line $r'$ at station $s$) |
| $\delta^{kk'}_{gr's}\in\{0,1\}$ | Denotes whether passenger group $g$ makes the transfer from the $k$th vehicle of line $r$ to the $k'$th vehicle of line $r'$ at station $s$ (an alternate form of the symbol, $\delta^{kk'}_{g\psi^{(i)}}$, with $\psi^{(i)}=\left(r^{(i)},r^{(i+1)},s^{(i)}\right)\in\Psi_g$ is also used for notational convenience) |
| $\delta^k_g\in\{0,1\}$ | Denotes whether boarding the $k$th vehicle of transit line $r_g^{(1)}$ is possible for passenger group $g$ at their origin $s_g^{(0)}$ |
| $z_g$ | Arrival time of passenger group $g$ at their destination $s_g^{(\lvert S_g\rvert-1)}$ |
| $w_g$ | Waiting time for passenger group $g$ at their origin $s_g^{(0)}$ |
| $v_g$ | Total in-vehicle time for passenger group $g$ |
| $p_g$ | Path transfer time for passenger group $g$ |
| $e_g$ | Time difference between $\underline{A}_g$ and $z_g$, if passenger group $g$ arrives earlier than expected (zero otherwise) |
| $l_g$ | Time difference between $z_g$ and $\overline{A}_g$, if passenger group $g$ arrives later than expected (zero otherwise) |

departure of the passengers on the next bus of the connecting route from the transfer station, $d^{k'}_{r's}$, as the transfer time $t^{kk'}_{rr's}$ ($C+D$ and $F+G$). For itineraries involving two or more transfers, the sum of all relevant transfer times are denoted as the path transfer time $p_g$ for passenger group $g$ ($C+D+F+G$).

In this work, we also keep track of the arrival time of the passengers at their destination denoted by $z_g$. This allows us to penalize early or late arrivals at their destinations. We assume that the headway range of these routes $\left[\underline{H}_r, \overline{H}_r\right]$ are published and communicated to the public. Based on that information, the passengers can estimate the expected time of arrival at their destination by the following:

$$F_g + \sum_{(r,r',s)\in\Psi_g}\left(W_{rr's} + \frac{\underline{H}_r+\overline{H}_r}{4}\right) + \sum_{(r,s,s')\in\Phi_g} T_{rss'} \tag{1}$$

where $\frac{\underline{H}_r+\overline{H}_r}{4}$ gives the approximated mean waiting time at each transfer stop, when only the headway range $\left[\underline{H}_r, \overline{H}_r\right]$ is made known to the public. $T_{rss'}$ is the mean in-vehicle travel time on segment $(r,s,s')$. We assume that passengers consider arriving within ten minutes of this expected arrival time as being on time and no penalty for early or late arrival shall be incurred. This time interval is denoted as $\left[\underline{A}_g, \overline{A}_g\right]$ for each passenger group.

The objective of the model is to provide travelers with a seamless travel experience. We do so by minimizing the weighted sum of all time-related attributes as follows:

$$\min \sum_{g\in G} Q_g\left(C_w w_g + C_v v_g + C_p p_g + C_e e_g + C_l l_g\right) \tag{2}$$

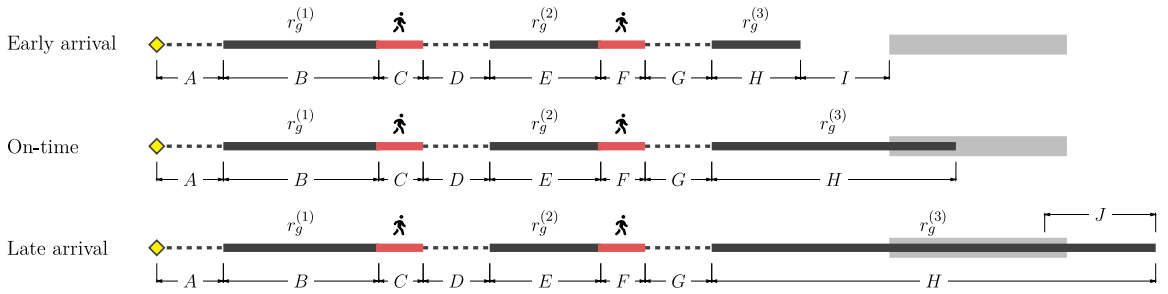


**Fig. 2.** The anatomy of three different types of itineraries. In all of these cases, the yellow diamond denotes the arrival of the passengers at the origin stop, dotted lines are the time spent waiting for a bus, black solid lines are time spent in the vehicle, red solid lines are time spent transferring between platforms of different routes at the same stop, and gray rectangle signifies the time range within which arrivals are considered to be on-time. In all three itineraries, path transfer time $p_g = C + D + F + G$ and $v_g = B + E + H$. The early arrivals $e_g$ for all three itineraries are $I$, 0 and 0 respectively, whereas late arrivals $l_g$ are 0, 0 and $J$ respectively. (For interpretation of the references to color in this figure legend, the reader is referred to the web version of this article.)

where $Q_g$ is the given demands, $w_g$ is the waiting time at the origin stop, $v_g$ is the total in-vehicle time, $p_g$ is the path transfer time, $e_g$ is the early arrival and $l_g$ is the late arrival for passenger group $g$. These variables are weighted by an estimate of the passengers' value of time during the different stages of the trip. The weights can also be calibrated to prioritize an attribute or a set of attributes over the others.

The objective function given by Eq. (2) could be extended to consider a general connectivity measure that captures other qualitative and quantitative attributes as established by Ceder and Teh (2010) and Ceder (2016). We focus only on time-related attributes, with the intention of examining the effect of time-dependent travel times on these attributes.

The constraints can be broadly classified into the following categories: operational (Section 3.3.3); related to the modeling of transfer time at a single stop (Section 3.3.4); related to the determination of passengers' itineraries (Section 3.3.5); related to path transfer time (Section 3.3.6); related to early and late arrivals (Section 3.3.7); and related to other time-related attributes (Section 3.3.8).

### 3.3.3. Operational constraints

The operational constraints include

$$\underline{H}_r \le d^1_{rs^{(1)}} \le \overline{H}_r \qquad \forall r \in R \quad (3)$$

$$d^{|K_r|}_{rs^{(1)}} \le \overline{D} \qquad \forall r \in R \quad (4)$$

$$\underline{H}_r \le d^{k+1}_{rs} - d^k_{rs} \le \overline{H}_r \qquad \forall r \in R \quad s \in S_r \setminus \{s_r^{(|S_r|)}\} \quad k \in K_r \setminus \{|K_r|\} \quad (5)$$

$$d^k_{rs} = a^k_{rs} + u^k_{rs} \qquad \forall r \in R \quad s \in S_r \setminus \{s_r^{(|S_r|)}\} \quad k \in K_r \quad (6)$$

$$\underline{U}_{rs} \le u^k_{rs} \le \overline{U}_{rs} \qquad \forall r \in R \quad s \in S_r \setminus \{s_r^{(|S_r|)}\} \quad k \in K_r \quad (7)$$

$$a^k_{rs^{(i)}} = d^k_{rs^{(i-1)}} + \sum_{\tau \in T} \varphi^{k\tau}_{rs^{(i-1)}} t^{\tau}_{rs^{(i-1)}} \qquad \forall r \in R \quad s^{(i-1)}, s^{(i)} \in S_r \quad k \in K_r \quad (8)$$

Constraint (3) states that the departure time of the first vehicle of each transit line $r$ from the terminal station $s_r^{(1)}$ should be within the allowable headway range. Constraint (4) dictates that the last trip of each route is to depart from the origin within the planning horizon $\overline{D}$. Constraint (5) limits the departure headway to be within $\left[\underline{H}_r, \overline{H}_r\right]$. Constraint (6) states that the departure time equals the sum of the arrival time, $a^k_{rs}$, and dwell time, $u^k_{rs}$. Constraint (7) defines the boundary of the dwell time.

When time-dependent travel time and flexible headway scheduling is considered, as in our case, the problem of bus bunching becomes relevant. Thus, we have to ensure that the allowable headway range $\left[\underline{H}_r, \overline{H}_r\right]$ and the allowable dwell time $\left[\underline{U}_{rs}, \overline{U}_{rs}\right]$ are set in a way that prevents bus bunching from happening. In particular, when we set the parameters such that $\overline{U}_{rs} < \underline{H}_r$, Constraint (5) and Constraint (7) would ensure that bunching does not occur.

Constraint (8) is the time-dependent arrival time constraint, which states the arrival time of the $k$th vehicle of transit line $r$ at station $s_r^{(i)}$ depends on the time window within which the vehicle departs the previous stop $s_r^{(i-1)}$. Throughout the formulation, the route indices are dropped from $s_r^{(i)}$ when the decision variable is indexed by the same route index $r$, e.g. $d^k_{rs^{(i)}}$ is equivalent to $d^k_{rs_r^{(i)}}$. $\varphi^{k\tau}_{rs}$ is a binary decision variable indicating whether or not the $k$th vehicle of line $r$ departs from stop $s$ within time window $\tau$. By definition, $\varphi^{k\tau}_{rs}$ can be determined by the following constraints:

$$\sum_{\tau \in T} \tau \vartheta \varphi^{k\tau}_{rs} \le d^k_{rs} < \sum_{\tau \in T} (\tau + 1) \vartheta \varphi^{k\tau}_{rs} \qquad \forall r \in R \quad s \in S_r \setminus \{s_r^{(|S_r|)}\} \quad k \in K_r \quad (9)$$

$$\sum_{\tau \in T} \varphi_{rs}^{k\tau} = 1 \qquad \forall r \in R \quad s \in S_r \setminus \{s_r^{(|S_r|)}\} \quad k \in K_r \tag{10}$$

$$\varphi_{rs}^{k\tau} \in \{0,1\} \qquad \forall r \in R \quad s \in S_r \setminus \{s_r^{(|S_r|)}\} \quad k \in K_r \quad \tau \in T \tag{11}$$

Constraint (9) states that if $\varphi_{rs}^{k\tau} = 1$, then the departure time is within time interval $[\tau\vartheta, (\tau+1)\vartheta)$. Constraint (10) means that the PT vehicle must depart from each stop exactly once within any time window. Constraint (11) states that $\varphi_{rs}^{k\tau}$ is a binary decision variable.

### 3.3.4. Transfer time at a single stop

In agreement with Wong et al. (2008), the following constraints determine the transfer time between two PT lines at a single station.

$$M\left(\Delta_{rr's}^{kk'} - 1\right) \le d_{r's}^{k'} - (a_{rs}^{k} + W_{rr's}) \le M\Delta_{rr's}^{kk'} \qquad \forall (r,r',s) \in \Psi \quad k \in K_r \quad k' \in K_{r'} \tag{12}$$

$$d_{r's}^{k'} - (a_{rs}^{k} - W_{rr's}) - M\left(\Delta_{rr's}^{kk'} - 1\right) \le t_{rr's}^{kk'} \qquad \forall (r,r',s) \in \Psi \quad k \in K_r \quad k' \in K_{r'} \tag{13}$$

$$\Delta_{rr's}^{kk'} \in \{0,1\} \qquad \forall (r,r',s) \in \Psi \quad k \in K_r \quad k' \in K_{r'} \tag{14}$$

where $M$ is a large positive number, $W_{rr's}$ is the minimum transfer time between lines $r$ and $r'$ at stop $s$. The minimum transfer time $W_{rr's}$ is an input parameter to capture the inevitable transfer time required such as the walking time between platforms of different transit lines. For transfers that require moving between two physical bus stops, e.g. street-crossing and sidewalk transfers as described in Hadas and Ranjitkar (2012), the walk time between the two stops can be estimated and incorporated in the same parameter. A buffer time can also be incorporated in $W_{rr's}$ to make the transfers more reliable and accommodating to people of reduced mobility.

$\Delta_{rr's}^{kk'}$ is a binary decision variable, and equals one if the transfer from the $k$th vehicle of transit line $r$ to the $k'$th vehicle of transit line $r'$ at station $s$ is feasible. A transfer is feasible if and only if the passenger on the $k$th vehicle of transit line $r$ arrives at the platform for the connecting route $r'$ at station $s$ no later than the departure time of the $k'$th vehicle of transit line $r'$ from station $s$ as defined in Constraint (12). The transfer time of each transfer is given by Constraint (13).

We note that a feasible transfer does not necessarily mean that travelers will use it. For example, if it is feasible for travelers to transfer to the $k'$th vehicle, then it is also feasible for travelers to transfer to the $(k'+1)$th vehicle. However, according to assumption A3, all passenger groups use only the first feasible transfer. This is formulated in the next subsection.

### 3.3.5. Determination of passengers' itineraries

The computation of the time-related attributes in the objective function requires the knowledge of the complete itinerary of each passenger, which in turn requires us to determine the buses that the passengers board at each leg of the trip. As stated in Section 3.2, the passengers are expected to always take the first bus available to them at each leg of the trip. Thus if we can determine the bus that the passengers board at the origin, we can deduce the same for subsequent legs using the same assumption.

We now introduce new binary variables $\delta_g^k$ to help us determine the bus that the passengers board at the origin. We use $\delta_g^k$ to denote if it is possible for travelers to board the $k$th vehicle of transit line $r_g^{(1)}$ at origin $s_g^{(0)}$. Mathematically, we can define $\delta_g^k$ as such:

$$\delta_g^k = \begin{cases} 1 & F_g \le d_{r_g^{(1)} s_g^{(0)}}^{k} \\ 0 & \text{otherwise} \end{cases} \qquad \forall g \in G \quad k \in K_{r_g^{(1)}} \tag{15}$$

Constraint (15) states that passenger group $g$ can board the $k$th vehicle, i.e. $\delta_g^k = 1$, if and only if their arrival at their origin station, $F_g$, is earlier than the departure time of the $k$th vehicle of transit line $r_g^{(1)}$ from stop $s_g^{(0)}$. Constraint (15) can be reformulated into the following constraints using the Big-M method.

$$d_{r_g^{(1)} s_g^{(0)}}^{k} - M\delta_g^k \le F_g \le d_{r_g^{(1)} s_g^{(0)}}^{k} - M\left(\delta_g^k - 1\right) \qquad \forall g \in G \quad k \in K_{r_g^{(1)}} \tag{16}$$

The following constraint then ensures that the passengers can board at least one vehicle of line $r_g^{(1)}$ at their origin, $s_g^{(0)}$.

$$\sum_{k \in K_{r_g^{(1)}}} \delta_g^k \ge 1 \qquad \forall g \in G \tag{17}$$

As discussed previously, we assume that the passengers always board the next bus that is available to them. Thus in order to determine the bus that the passengers board at their origin, we ought to look at $\delta_g^k$ of neighboring buses. At this juncture we should recognize the fact that the passengers would board the $k$th vehicle of transit line $r$ if and only if $\delta_g^k = 1$ and $\delta_g^{k-1} = 0$. We have established in Constraint (15) that $\delta_g^k$ should only be set to one if and only if the passengers arrive earlier than the departure of the

$k$th bus, and from Constraint (5) we know that the buses cannot overtake each other, thus by induction when $\delta_g^{k-1} = 0$ then there can never be $\dot{k} < k-1$ such that $\delta_g^{\dot{k}} = 1$, and that the $k$th bus would be the next available bus to passenger group $g$.

Now that we have determined the bus that the passengers board at the origin, we shall focus on subsequent legs of the trip. Before we do that, we need to introduce new binary variables $\delta^{kk'}_{g\psi^{(i)}}$ to denote if the passenger group $g$ makes the transfer from the $k$th vehicle of transit line $r_g^{(i)}$ to the $k'$th vehicle of transit line $r_g^{(i+1)}$ at transfer stop $s_g^{(i)}$. These transfer decisions will naturally depend on the buses that the passengers boarded in the legs before them, tracing all the way back to the first leg. We model the decisions with the following constraints:

$$\delta^{kk'}_{g\psi^{(1)}} = \begin{cases} 1 & \delta_g^k - \delta_g^{k-1} = 1, \Delta^{kk'}_{\psi^{(1)}} - \Delta^{k(k'-1)}_{\psi^{(1)}} = 1 \\ 0 & \text{otherwise} \end{cases} \qquad \forall g \in G \quad k \in K_{r_g^{(1)}} \quad k' \in K_{r_g^{(2)}} \tag{18}$$

$$\sum_{j \in K_{r^{(i)}}} \sum_{j' \in K_{r^{(i+1)}}} \delta^{jj'}_{g\psi^{(i)}} = 1 \qquad \forall g \in G \quad \psi^{(i)} = \left(r^{(i)}, r^{(i+1)}, s^{(i)}\right) \in \Psi_g \tag{19}$$

Constraint (18) gives the condition for deciding the buses to board for the first two legs of the trips. The first condition $\delta_g^k - \delta_g^{k-1} = 1$, as we have discussed earlier in this section, ensures that the passengers board the next available bus at the origin. The next condition $\Delta^{kk'}_{\psi^{(1)}} - \Delta^{k(k'-1)}_{\psi^{(1)}} = 1$ lays the requirement for selecting the $k'$th bus for route $r_g^{(2)}$ having selected the $k$th bus for route $r_g^{(1)}$. In Section 3.3.4, we have established that if the transfer from $k$th vehicle of transit line $r_g^{(1)}$ to the $k'$th vehicle of transit line $r_g^{(2)}$ at stop $s_g^{(1)}$ is possible, i.e. $\Delta^{kk'}_{\psi^{(1)}} = 1$, then the transfers to the $\dot{k}$th vehicle of transit line $r_g^{(2)}$ for $\dot{k} > k'$ would also be possible, i.e. $\Delta^{kk}_{\psi^{(1)}} = 1$. Hence, in order to ensure that the passengers board the next available bus, the condition $\Delta^{kk'}_{\psi^{(1)}} - \Delta^{k(k'-1)}_{\psi^{(1)}} = 1$ is added. Note that in Constraint (18), the terms $\delta_g^{k-1}$ and $\Delta^{k(k'-1)}_{\psi^{(1)}}$ should be dropped when they are undefined, e.g. when $k = 0$ or $k' = 0$. The conditions in Constraint (18) can be reformulated as follows:

$$\delta^{kk'}_{g\psi^{(1)}} \geq \left(\delta_g^k - \delta_g^{k-1}\right) + \left(\Delta^{kk'}_{\psi^{(1)}} - \Delta^{k(k'-1)}_{\psi^{(1)}}\right) - 1 \qquad \forall g \in G \quad k \in K_{r_g^{(1)}} \quad k' \in K_{r_g^{(2)}} \tag{20}$$

$$\delta^{kk'}_{g\psi^{(1)}} \leq \delta_g^k - \delta_g^{k-1} \qquad \forall g \in G \quad k \in K_{r_g^{(1)}} \quad k' \in K_{r_g^{(2)}} \tag{21}$$

$$\delta^{kk'}_{g\psi^{(1)}} \leq \Delta^{kk'}_{\psi^{(1)}} - \Delta^{k(k'-1)}_{\psi^{(1)}} \qquad \forall g \in G \quad k \in K_{r_g^{(1)}} \quad k' \in K_{r_g^{(2)}} \tag{22}$$

Note that the terms $\delta_g^{k-1}$ and $\Delta^{k(k'-1)}_{\psi^{(1)}}$ in Constraints (20) through (22) should also be dropped when they are undefined, as in Constraint (18).

Having decided the buses to board up to the first transfer, Constraint (19) would suffice to decide the buses to board for subsequent legs of the trip. Though Constraint (19) only ensures that one pair of buses $(j, j')$ is selected for each transfer $\psi^{(i)}$, the minimization of the objective function in Eq. (2) would guarantee that the next available bus is selected for each subsequent leg. With all the constraints introduced in this section, we have successfully determined the complete itinerary of each passenger group. In the section that follows, we shall use the results from this section to define the time attributes that appeared in the objective function.

### 3.3.6. *Path transfer time and initial waiting time at origin*

Using $t^{kk'}_{rr's}$ and $\delta^{kk'}_{g\psi^{(i)}}$ defined in Sections 3.3.4 and 3.3.5 respectively, the path transfer time for passenger group $g$ can be defined as:

$$p_g = \sum_{\psi^{(i)}=\left(r^{(i)}, r^{(i+1)}, s^{(i)}\right) \in \Psi_g} \sum_{k \in K_{r^{(i)}}} \sum_{k' \in K_{r^{(i+1)}}} \delta^{kk'}_{g\psi^{(i)}} t^{kk'}_{\psi^{(i)}} \qquad \forall g \in G \tag{23}$$

In order to provide PT travelers with a smooth travel experience, the following maximum path transfer time constraint is imposed,

$$p_g \leq \overline{P}_g \qquad \forall g \in G \tag{24}$$

where $\overline{P}_g$ is the maximum allowable path transfer time for passenger group $g$.

In this study, we do not explicitly impose an upper bound to limit the number of transfers of each passenger. Instead, we can achieve a similar effect by imposing an upper bound to the path transfer time. Itineraries with many transfers are likely to have longer transfer times accumulated from each transfer, thus imposing a maximum path transfer time could achieve a similar effect in limiting the number of transfers. We recognize that the two constraints are not identical, and there exists a possibility that an itinerary be made up of multiple short transfers. This motivates our contribution in this study, in that, we consider the transfer experience of the trip as a whole, and not only by considering the number of transfers. In fact, a trip that is made up of multiple short transfers does not necessarily equate to having long path transfer time, and transit users may well be accepting towards trips with more transfers when they are well-planned and coordinated (Allen et al., 2019). By doing so, we allow, up to a certain extent, an itinerary to contain a reasonable number of transfers if the overall transfer experience measured by the path transfer time is acceptable.

### 3.3.7. Early and late arrival at destination

As discussed previously in Section 3.3.2, we assume that the headway range is published and made known to the passengers such that the passengers can work out a time interval within which they can expect to arrive at their destination. With the publication of such information, passengers have a higher tendency of planning ahead such that they can arrive at their destination on time. Therefore, it is important that we keep track of the time at which the passengers arrive at their destination, and penalize accordingly if any passenger arrives outside the expected time interval. Both early and late arrivals should be penalized, although the penalty for late arrivals would be higher in most cases. We introduce three variables $z_g$, $e_g$ and $l_g$ to keep track of the values that we are interested in.

$$z_g \geq M\left(\delta^{kk'}_{g\psi^{(|\Psi_g|)}} - 1\right) + a^{k'}_{r_g^{(|R_g|)}\, s_g^{(|S_g|-1)}} \qquad \forall g \in G \quad k \in K_{r_g^{(|R_g|-1)}} \quad k' \in K_{r_g^{(|R_g|)}} \tag{25}$$

$$e_g \geq \underline{A}_g - z_g \qquad \forall g \in G \tag{26}$$

$$l_g \geq z_g - \overline{A}_g \qquad \forall g \in G \tag{27}$$

Constraint (25) defines $z_g$, which represents the arrival time of the passengers at their destination $s_g^{(|S_g|-1)}$ on route $r_g^{(|R_g|)}$. When the passengers do not make the transfer from the $k$th bus to the $k'$th bus on their last transfer $\psi^{(|\Psi_g|)}$, i.e. $\delta^{kk'}_{g\psi^{(|\Psi_g|)}} = 0$, then the right hand side of Constraint (25) would become a large negative number and the constraint becomes non-binding. However, when $\delta^{kk'}_{g\psi^{(|\Psi_g|)}} = 1$, Constraint (25), together with the minimization of the objective function, sets $z_g$ exactly to the arrival of the passengers at their destination.

Constraint (26) and Constraint (27) together with the non-negativity constraints define the variables $e_g$ and $l_g$, which represent the margin of early and late arrivals respectively. When the passengers arrive earlier than expected, i.e. $z_g \leq \underline{A}_g$, Constraint (26), together with the minimization of the objective function, sets $e_g$ exactly to the difference $\underline{A}_g - z_g$. Similarly, when the passengers arrive later than expected, i.e. $z_g \geq \overline{A}_g$, Constraint (27), together with the minimization of the objective function, sets $l_g$ exactly to the difference $z_g - \overline{A}_g$.

### 3.3.8. Accounting of other time-related attributes

Although the aim was to provide a more seamless transfer experience to the passengers, the other time-related attributes of a trip have to be accounted for, as indicated in the objective function Eq. (2). This is done in order to prevent the other time-related attributes from being severely compromised in favor of a near-perfect transfer experience. In this section, we shall present the constraints that help to keep track of the waiting time at the origin $w_g$ and total in-vehicle travel time $v_g$.

In Section 3.3.5, we have defined the variable $\delta^k_g$ to keep track of the bus that the passengers board at the origin stop $s_g^{(0)}$. The only thing left to do is to associate the waiting time of the passengers at the origin stop $w_g$, with the appropriate bus arrival time.

$$w_g \geq M\left(\delta^k_g - \delta^{k-1}_g - 1\right) + \left(a^k_{r_g^{(1)} s_g^{(0)}} - F_g\right) \qquad \forall g \in G \quad k \in K_{r_g^{(1)}} \tag{28}$$

When a passenger boards the $k$th vehicle of transit line $r_g^{(1)}$, i.e. $\delta^k_g = 1$, then by assumption $\delta^{k-1}_g = 0$ (see Item A3 of Section 3.2 and Section 3.3.5). In this case, the first term on the right-hand side of Constraint (28) is negated, and through the minimization of the objective function, $w_g$ is set to the difference between the arrival time of $k$th vehicle of transit line $r_g^{(1)}$ at the origin $s_g^{(0)}$ and the passengers' time of arrival at the origin $F_g$. Note that the first term can only be negated as such, as we shall see in the following exposition that all other combinations of $\delta^k_g$ and $\delta^{k-1}_g$ would lead to the same conclusion.

In the case where boarding the $k$th bus is not possible but boarding the $(k-1)$th bus is possible, the difference $\delta^k_g - \delta^{k-1}_g$ is $-1$, whereas in the case where boarding of both the $k$th and $(k-1)$th buses are not possible, the difference becomes 0. In both of these cases, the right-hand side becomes a large negative number and the relevant constraints shall not be binding. Note that, as in Constraint (18) and Constraints (20) through (22), $\delta^{k-1}_g$ should be dropped from Constraint (28) when it is undefined, i.e. $k = 0$.

The total in-vehicle time $v_g$ can be inferred from the transfer decision variables $\delta^{kk'}_{grr's}$ and the arrival and departure times of the buses concerned. However, we could also calculate the in-vehicle time by subtracting the waiting time at the origin stop $w_g$ and path-transfer-time $p_g$ form the trip duration given by $z_g - F_g$ (see Fig. 2 for an illustration of an itinerary). Mathematically, we can write the following:

$$v_g = (z_g - F_g) - w_g - p_g \qquad \forall g \in G \tag{29}$$

With that, we have fully defined all components of the objective function in Eq. (2).

## 4. Valid inequalities

The model developed in the previous section is a mixed integer linear programming problem (MILP) and can be solved using existing commercial solvers, such as CPLEX. In order to accelerate the computation for real applications, three valid inequalities (VIs) are proposed in this study. Valid inequalities, also known as cuts, are constraints that do not eliminate any feasible integer

solutions, but could reduce the computation time by reducing the size of the feasible region (Wolsey, 1998). In this study, the VIs are derived based on the properties of the problem and its formulation. The valid inequalities can be added into the model in either of two ways, i.e. added as regular constraints of the model or implemented within a branch and cut framework. We shall discuss and compare the two options further in Section 5.2.3.

Intuitively, the first VI is based on the fact that if a transfer is feasible, then the gap between the departure and arrival times should be greater than the minimum transfer time. The second VI is motivated by the maximum path-transfer time constraint, which restricts the transfer time at each stop to be less than the maximum path transfer time. The idea of the third VI is similar to the first VI, but focuses on the integrality condition of the decision variables. Finally, the last two VIs extend the work by Fouilhoux et al. (2016); see this work for more details.

### 4.1. Headway inequalities

This family of valid inequalities relate the feasibility of each transfer to the maximum and minimum allowable headway of the connecting routes. The valid inequalities are given as follows:

$$d^{|K_{r'}|}_{r's} - \sum_{i=k'}^{|K_{r'}|} \Delta^{ki}_{rr's}\overline{H}_{r'} - (a^{k}_{rs} + W_{rr's}) < M\Delta^{kk'}_{rr's} \qquad \forall (r,r',s) \in \Psi \quad k \in K_r \quad k' \in K_{r'} \quad \text{(VI-1)}$$

The right-hand side of the inequality indicates whether, or not, a transfer is feasible. The left-hand side term is the gap between two timestamps. The term in the parentheses is the arrival time of passengers traveling on the $k$th vehicle of transit line $r$ , at the platform of route $r'$ at station $s$, whereas the remaining left-hand side terms give the earliest possible departure time of a vehicle of transit line $r'$ from station $s$. If this gap is positive, i.e. passengers' arrival at the transfer platform is before the earliest possible departure time of the connecting bus, then the transfer is feasible, and vice versa. The proof for the VI is given in Appendix A.

### 4.2. Maximum path transfer time inequalities

This family of valid inequalities are derived based on the relationship between the transfer decision of each passenger group and the maximum path transfer time. The inequalities are given as follows:

$$a^{k}_{rs} + W_{rr's} + \overline{P}_g\left(1 - \delta^{kk'}_{grr's}\right) - d^{\dot{k}'}_{r's} + \sum_{i=r'}^{\dot{k}'} \Delta^{kk'}_{rr's}\overline{H}_{r'} > M\left(\delta^{kk'}_{grr's} - 1\right) \qquad \forall (r,r',s) \in \Psi \quad k \in K_r \quad k', \dot{k}' \in K_{r'} \quad \dot{k}' \geq k' \quad \text{(VI-2)}$$

The right-hand side of the VI indicates whether, or not, a group of passengers makes the transfer from the $k$th vehicle of transit line $r$ to the $k'$th vehicle of transit line $r'$ at station $s$, where the left-hand side of the VI expresses the difference between the maximum path transfer time and the transfer time at a single stop. We present a rigorous proof of the VI in Appendix B.

### 4.3. Departure decision inequalities

In this section, we derive valid inequalities based on the departure decisions of transit lines $r$ and $r'$ from each stop. The valid inequalities are stated as follows:

$$\Delta^{kk'}_{rr's} \leq \max\left(0, \frac{\Lambda}{W_{rr's}}\right) \qquad \forall (r,r',s) \in \Psi \quad k \in K_r \quad k' \in K_{r'} \quad \text{(VI-3)}$$

$$\Lambda = \left(a^{k'}_{r's(0)} + \sum_{j=0}^{i}\sum_{\tau\in T}\varphi^{k'\tau}_{r's(j)}t^{\tau}_{r's(j)} + \sum_{j=0}^{i}u^{k'}_{r's(j)}\right) - \left(a^{k}_{rs(0)} + \sum_{j=0}^{i}\sum_{\tau\in T}\varphi^{k\tau}_{rs(j)}t^{\tau}_{rs(j)} + \sum_{j=0}^{i-1}u^{k}_{rs(j)}\right)$$

The term $\Lambda$ computes the difference between the departure time of the $k'$th vehicle of transit line $r'$ and the arrival time of the $k$th vehicle of transit line $r$ . When the difference is greater than $W_{rr's}$, or equivalently, its quotient is greater than one, then the transfer between the two vehicles is feasible and the corresponding binary variable $\Delta^{kk'}_{rr's}$ can be equal to one. We provide a proof of the VI in Appendix C.

### 4.4. Fouilhoux et al.'s synchronization and headway inequalities (Fouilhoux et al., 2016)

Fouilhoux et al. (2016) developed two classes of valid inequalities for the transfer synchronization problem. The problem addressed in their study, however, is slightly different than the one discussed in this paper. The objective of their study was to maximize the number of synchronized transfers across the network, whereas ours is to minimize the total path transfer time of all passengers. Therefore, in Fouilhoux et al. (2016), it suffices to define the synchronization variables, whose values depend on whether or not the difference between the arrival times of the connecting vehicle and its previous vehicle falls within a predetermined range

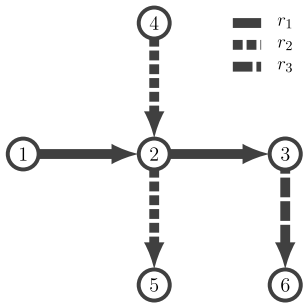


| PG | Path | Arr. |
|---|---|---|
| 1 | (1) $\xrightarrow{r_1}$ (3) $\xrightarrow{r_3}$ (6) | 9 |
| 2 | (4) $\xrightarrow{r_2}$ (2) $\xrightarrow{r_1}$ (3) $\xrightarrow{r_3}$ (6) | 7 |
| 3 | (1) $\xrightarrow{r_1}$ (2) $\xrightarrow{r_2}$ (5) | 10 |

**Fig. 3.** An illustrative example of time-dependent travel times.

of values known as the *waiting time window*. The lower bound of the waiting time window ensures that the passengers have sufficient time to transfer between platforms of the different transit lines. The upper bound, on the other hand, sets the limit to the waiting time of the passengers at the transfer stations. In this study, however, on top of the knowledge of whether a transfer is synchronized, we ought to know which transfers the passengers are making in order to calculate the transfer time incurred for each passenger group. Thus, the variables are defined slightly different here. We define the transfer decision variables, $\delta^{kk'}_{grr's}$, to determine if a passenger group makes a certain transfer. Nevertheless, similar to Fouilhoux et al. (2016), in order for a passenger group to make a transfer, our study still requires that the arrival times of the two vehicles involved in the transfer have to satisfy the synchronization time window condition. Therefore, the synchronization inequalities proposed in Fouilhoux et al. (2016) can be adapted to our model by substituting the synchronization variables in their study with the transfer decision variables defined in our study, $\delta^{kk'}_{grr's}$, as follows:

$$\sum_{k\in K_{r'}} \delta^{kk}_{grr's} \le 1 + \left\lfloor \frac{\overline{P}_g - W_{rr's}}{\underline{H}_{r'}} \right\rfloor \qquad \forall g \in G \quad (r,r',s) \in \Psi_g \quad k \in K_r \quad \text{(VI-4A)}$$

$$\sum_{k\in K_r} \delta^{kk'}_{grr's} \le 1 + \left\lfloor \frac{\overline{P}_g - W_{rr's}}{\underline{H}_{r}} \right\rfloor \qquad \forall g \in G \quad (r,r',s) \in \Psi_g \quad k' \in K_{r'} \quad \text{(VI-4B)}$$

Here, the lower and upper bounds for the arrival time difference between vehicles of two transit lines are given by the minimum transfer time between platforms $W_{rr's}$ and the maximum path transfer time $\overline{P}_g$ respectively. We refer interested readers to Fouilhoux et al. (2016) for a proof of validity of these valid inequalities as they are very similar.

Similarly, we can adapt the headway inequalities to our model by replacing the synchronization variables with transfer decision variables to obtain the follow valid inequalities:

$$\delta^{kk'}_{grr's} + \sum_{k=k'+1}^{|K_{r'}|} \delta^{kk}_{grr's} + \sum_{k=k+1}^{|K_r|} \delta^{kk}_{grr's} \le 1 + \left\lfloor \frac{\overline{P}_g - W_{rr's}}{\min\left(\underline{H}_r, \underline{H}_{r'}\right)} \right\rfloor \qquad \forall g \in G \quad (r,r',s) \in \Psi_g \quad k \in K_r \quad \text{(VI-5A)}$$

$$\delta^{kk'}_{grr's} + \sum_{k=1}^{k'-1} \delta^{kk}_{grr's} + \sum_{k=1}^{k-1} \delta^{kk}_{grr's} \le 1 + \left\lfloor \frac{\overline{P}_g - W_{rr's}}{\min\left(\underline{H}_r, \underline{H}_{r'}\right)} \right\rfloor \qquad \forall g \in G \quad (r,r',s) \in \Psi_g \quad k \in K_r \quad \text{(VI-5B)}$$

## 5. Numerical studies

In this section, we first demonstrate the key novelties of this study using a small artificial network. In particular, we show in Section 5.1.1 how the use of time-dependent travel data can help us obtain transit schedules that are more representative of the true traffic conditions, which in turn reduces the passengers' overall trip time. We also show in Section 5.1.2 that there exists a tradeoff between the maximum allowable path transfer time and the overall trip times.

Next, we use a real-world dataset to evaluate the optimized schedules and also the performance of the valid inequalities. We compare the time-related attributes of the trips under the optimized and non-optimized schedules in Section 5.2.1. Finally, we present the performance of the valid inequalities in Section 5.2.2 and the comparison for two different strategies for the implementation of the valid inequalities in Section 5.2.3.

### 5.1. Evaluation on small artificial network

The network defined in Fig. 3 contains three PT lines marked with different line styles and three passenger groups. The itinerary of each passenger group is given in the table of Fig. 3. In this example, it is assumed that the time-dependent travel time is the real travel time, and we compare the non-optimized schedule, schedule optimized using time-independent mean travel time data and schedule optimized using time-dependent travel time data.

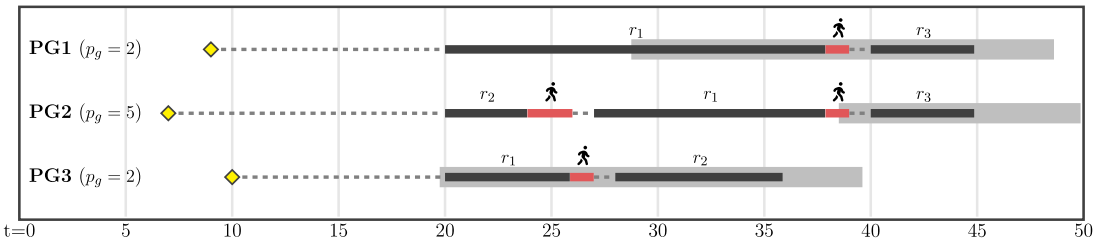


(a) Itineraries of three passenger groups under the non-optimized constant headway schedule.

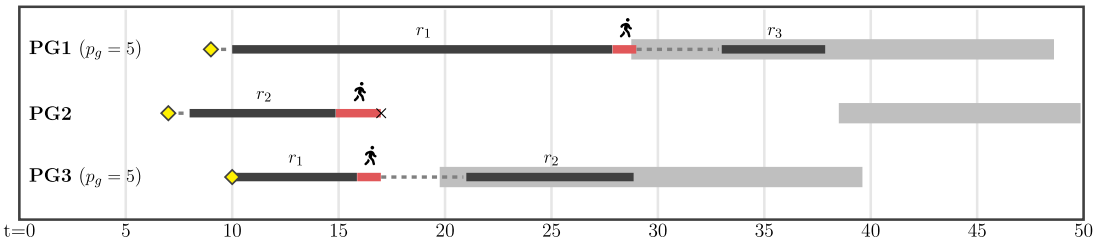


(b) Itineraries of three passenger groups under the schedule optimized with mean travel time data.

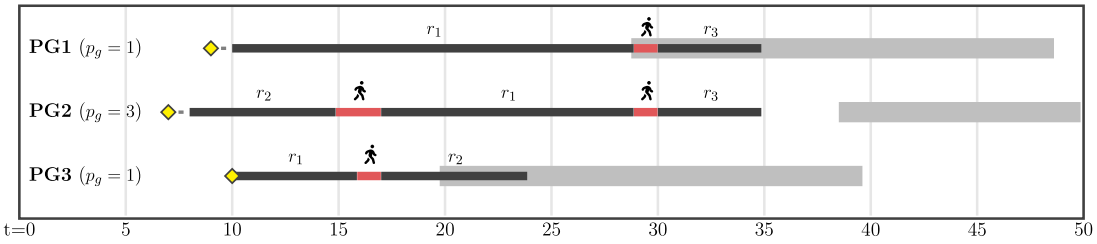


(c) Itineraries of three passenger groups under the schedule optimized with time-dependent travel time data.

**Fig. 4.** Itineraries of passengers under different schedules. The cross marks ("X") indicate that the passengers are not able to complete their trip with the buses that are considered within the current planning horizon. However, this does not mean that the passengers can never complete the trip and are left stranded at the transfer stops. The passengers may be able to connect to other buses within the next planning horizon and incur longer waiting times and arriving later than expected.

For a fair comparison, the time-independent travel time used is derived from the average of time-dependent link travel time used in the former. This emulates the scenario in which the average travel time is used in place of the time-dependent travel time due to a lack of temporal resolution in the available data, which is often the case in the transit scheduling literature.

*5.1.1. Benefits of schedule optimization using time-dependent travel time data*

In this section, we demonstrate that it is beneficial for transit operators to optimize transit schedules in a way that enhances the passengers' overall travel experience. We also show that the use of time-dependent travel time data is important when the optimization of schedules is considered. The input parameters and the experiment setup for this section are documented in Appendix D.

Fig. 4 shows passenger itineraries under different schedules. Fig. 4(a) shows the passengers' itineraries under the non-optimized schedule, which is obtained by subjecting the vehicles to a constant headway over the planning horizon. Under the constant headway schedule, passengers can expect to wait for a period of time that is proportional to the service headways for the bus to arrive at their origins. The passengers can also expect to do the same at the transfer stops. Each leg of the trip can in fact be considered independent of each other for each passenger because the services are not synchronized. As a result, the overall travel experience would be inversely related to the number of transfers involved, especially when the service frequencies are low.

In Fig. 4(b), we subject the passengers to the schedule optimized using time-independent travel time data, i.e. the mean travel time over the planning horizon. We note that in the figure we placed cross marks ("X") in to indicate that the passengers are not able to complete the trip because of missed transfers. This happens because we are considering a finite number of trips within a finite planning horizon. The passengers may be able to transfer to a bus within the next planning horizon and complete the trip, but not with the buses within the current planning horizon. This problem can be eradicated by extending the planning horizon to consider larger and indeterministic number of trips in the model, making it more complex and possibly intractable model. Nevertheless, there is no need to do so because, by definition, these trips falling within the extended time span will be characterized by longer wait times (low frequency service) in comparison to the trips within the original planning horizon. Under this schedule, the waiting times at their respective origins are significantly reduced. However, compared to Fig. 4(a), the path transfer times for PG1 and PG3

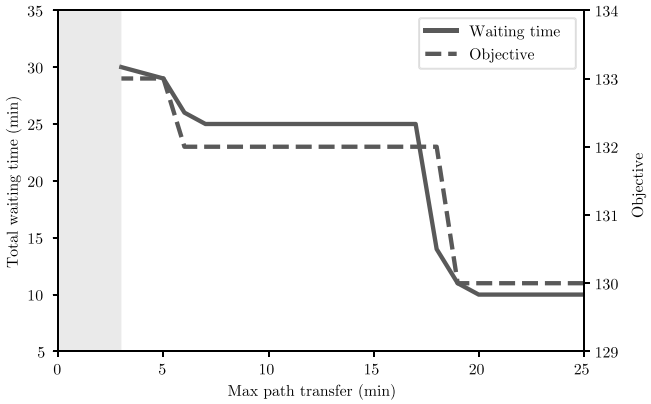


**Fig. 5.** Tradeoff between maximum path transfer time and objective value.

have increased significantly, whereas PG2 cannot complete their trip within the planning horizon. From the itineraries in Fig. 4(b), it becomes evident that optimizing the schedules using time-independent mean travel time data can sometimes do more harm than good.

Finally, in Fig. 4(c) we show the passengers' itineraries subjected to the schedule optimized using time-dependent travel time data. In this case, not only are the waiting times at the origin are reduced, the waiting times at the transfer stops are significantly reduced. More importantly, the passengers are able to complete their trips within the planning horizon, which means that the overall trip times are also considerably shorter than the case where the trips could only be completed in the next planning horizon (e.g. PG2 in Fig. 4(b)). The improvement observed under this schedule can be attributed to the use of time-dependent travel time data, which is more representative of the true travel times than the mean travel time used in Fig. 4(b).

In both cases where the schedules are opportunistically optimized to enhance the passengers' travel experience, we can expect the waiting times at the transfer stops to be low. This means that there will be a smaller margin for error when something in the system does not work as expected, e.g. travel time estimation errors, service disruptions and so forth. When data that is not representative of the true conditions are used (e.g. mean travel time data), instead of synchronizing the schedules, we run the risk of systematic desynchronization which leads to worse travel experience (Liu and Miller, 2020). Therefore, when such optimizations are performed, it is in the transit planners' best interest to acquire relevant data at the highest possible resolution and accuracy.

#### *5.1.2. Effects of path transfer time constraint*

Fig. 5 shows that there is a tradeoff between the maximum path transfer time and the objective function value. Mathematically, this is because a lower maximum path travel time imposes a tighter constraint on the optimization problem which results in a higher objective function value. As the constraint on maximum path travel time becomes tighter, one would reach a point at which the problem becomes infeasible. In this case, the minimum transfer time between certain stops are 3 minutes, hence, any threshold to the path transfer time set below this value would render the problem infeasible.

### *5.2. Evaluation on real-world transit dataset*

In Section 5.1, we have established that the use of time-independent travel time data in schedule synchronization may have adverse effects on passengers' travel experience, and possibly effects that are completely the opposite of what is expected. Thus in this section, we consider the use of time-dependent travel time data in the schedule synchronization problem on a real-world dataset. In particular, we use the Danish Rejsekort smart card dataset involving three bus lines in Metropolitan Copenhagen, Denmark (as shown in Fig. 6) to evaluate the schedules optimized using time-dependent travel time data, and the performance of the valid inequalities. For benchmarking purposes, we also compare the passengers' itineraries under the optimized schedule to that under a constant headway schedule. The three bus lines, with line numbers 1A, 2A, and 3A respectively, are among the major bus lines in Copenhagen.

The Danish Rejsekort smart card dataset used in this work contains tap-in and tap-out records of passengers boarding and alighting trains and buses within the network. Each record is associated with a timestamp, boarding or alighting station, transit line used, and an anonymized identifier of the fare card. Using these information, we are able to infer trips taken by the passengers. The dataset, however, has a low data observability of approximately 30%. A big portion of data from commuters using alternative payment methods such as a smartphone app, paper tickets or seasonal passes, are not accounted for in this dataset. As a result, we have resorted to generating demand scenarios based on the dataset at hand in an attempt to recover the 70% of data that is not observable in the dataset.

Each demand scenario generated is defined by the following information: the number of passengers, the origin and destination stations of each passenger, the transit lines and transfer stations used by each passenger, and the time of arrival of the passenger at


**Fig. 6.** The three major bus lines used to evaluate the schedules optimized using time-dependent travel time data, and the performance of the proposed valid inequalities.

the origin. This case study concerns only passenger trips with at least one transfer between the three transit lines. Hence, trips that do not involve any transfers are discarded. For each scenario, the origin, destination, transfer stations, and transit lines used are sampled from probability distributions constructed using the Rejsekort data, whereas the passengers' arrival times at their origins are generated using a Poisson arrival process as in previous works in the literature (Toledo et al., 2010; Dessouky et al., 2003). The arrival rate is given by the average rate of passenger arrivals observed in the dataset, corrected using a multiplicative factor in order to account for the non-observable data.

Eight scenarios were generated for this case study, each of which covers a one-hour peak period between 8:00 a.m. and 9:00 a.m. In all of these scenarios, the prediction interval is 15 min, i.e. the travel time data remains constant throughout the 15 min time interval. The number of trips involving at least one transfer between any two transit lines averages at 22.75 trips per hour across all generated scenarios. The generated scenarios can be accessed at https://github.com/leeke2/tt-sync-scenarios.

We use the eight scenarios to compare the passengers' itineraries under the constant headway and optimized schedules in Section 5.2.1. In Section 5.2.2, the schedules of the transit lines are then optimized for each demand scenario with and without valid inequalities in order to compare the performance of each valid inequality and their combinations. Finally, in Section 5.2.3 we compare the addition of these valid inequalities as regular constraints in the model and as user cuts within a branch and cut framework.

The maximum computation time for each optimization is set to two hours. All computations are performed in a high-performance computing environment, where each optimization uses a single node equipped with two Intel® Xeon® Processor E5-2690 v3 processors and 128 GB of random access memory (RAM). We refer the readers to Appendix E for all the parameters used for the experiments.

### *5.2.1. Passengers' itineraries under constant headway and optimized schedules*

We present a comparison of the summary statistics of all time-related attributes under the optimized and non-optimized schedules in Table 2. We can observe that the use of time-dependent travel time data has resulted in significant improvements. In particular, the waiting time at origin, path transfer time and late arrivals decreased by about 78% on average, whereas the in-vehicle travel time decreased by 13.4%. The proportion of trips with late arrivals have decreased by 33.3 percentage points from 79.8% to 46.5%, whereas the proportion of trips that cannot be completed due to missed transfers is down to zero from 16.1%. In short, the benefits of using time-dependent data in the synchronization of schedules is apparent, as we can see from the significant improvements in all of the time-related attributes.

We noted in Section 3.2 the travel time is assumed to be deterministic for practical reasons, in comparison with being stochastic in the real-world. Although we do not explicitly consider the stochasticity of travel time in our model, we can incorporate some robustness to its uncertainty by means of tuning the minimum transfer time $W_{rr's}$. In Table 3, optimal schedules are shown for four scenarios that differ only by their different minimum transfer time. The optimized schedules are then evaluated against five realizations of travel time data generated by subjecting the mean time independent travel time data to randomly generated noise. As the result, in Table 3, the proportion of invalid trips for each of the scenarios decreases with the increase of the minimum transfer time. This suggests that larger minimum transfer times tend to be more robust to uncertainties of the travel time.

**Table 2**
Summary statistics of passengers' itineraries under optimized (Opt., using time-dependent travel time data) and non-optimized constant headway (NOpt.) schedules.

| Scenario | | Wait | I. Veh. | Walk | P. Trf. | Early | % Early | Late | % Late | % Inv. |
|---|---|---|---|---|---|---|---|---|---|---|
| S1 | NOpt. | 14.2 | 44.5 | 2.0 | 7.1 | - | - | 21.6 | 80.0 | 5.0 |
| | Opt. | 3.5 | 33.6 | 2.0 | 2.4 | - | - | 0.9 | 15.0 | - |
| S2 | NOpt. | 16.9 | 47.4 | 2.0 | 9.0 | - | - | 19.4 | 90.5 | - |
| | Opt. | 5.0 | 44.0 | 2.0 | 3.1 | - | - | 10.2 | 47.6 | - |
| S3 | NOpt. | 17.0 | 42.6 | 2.0 | 13.7 | - | - | 17.6 | 80.0 | 20.0 |
| | Opt. | 4.5 | 38.0 | 2.0 | 3.4 | - | - | 5.4 | 44.0 | - |
| S4 | NOpt. | 21.2 | 52.1 | 2.0 | 15.3 | - | - | 28.6 | 95.6 | - |
| | Opt. | 4.4 | 42.6 | 2.0 | 2.6 | - | - | 4.4 | 60.9 | - |
| S5 | NOpt. | 17.5 | 48.9 | 2.0 | 10.9 | - | - | 20.7 | 100.0 | - |
| | Opt. | 7.7 | 47.7 | 2.0 | 3.9 | - | - | 10.8 | 92.3 | - |
| S6 | NOpt. | 40.8 | 62.7 | 2.0 | 35.3 | - | - | 55.8 | 85.0 | 15.0 |
| | Opt. | 5.2 | 44.6 | 2.0 | 4.0 | - | - | 7.2 | 55.0 | - |
| S7 | NOpt. | 41.9 | 28.8 | 2.0 | 36.0 | - | - | 38.9 | 36.4 | 59.1 |
| | Opt. | 4.2 | 30.9 | 2.0 | 2.3 | - | - | 2.4 | 27.3 | - |
| S8 | NOpt. | 39.9 | 52.2 | 2.0 | 34.8 | - | - | 46.2 | 70.6 | 29.4 |
| | Opt. | 3.8 | 40.3 | 2.0 | 2.6 | - | - | 8.0 | 29.4 | - |
| Avg % Diff. | | -77.8 | -13.4 | 0.0 | -78.4 | 0.0 | 0.0 | -76.0 | -33.3 | -16.1 |

All time values are given in minutes. Wait: Waiting time, I. Veh.: In-vehicle travel time, Walk: Total walking time between platforms of different routes at transfer stations, P. Trf. Path transfer time, Early, Late: Average time margin for passengers arriving earlier or later than the interval of expected arrival respectively, % Early, % Late: Proportion of passengers arriving earlier or later than expected respectively, % Inv.: Proportion of passengers who cannot complete their trip with the buses that are considered within the planning horizon. The final row indicates the percentage difference of each metric between the optimized and non-optimized schedules. In other words, more negative numbers indicate larger improvements with the use of time-dependent travel time data. The hyphens (-) are used in place of zero for legibility reasons.

**Table 3**
Summary statistics of passengers' itineraries under optimized (Opt., using time-dependent travel time data) schedules under different minimum transfer times. All time values are given in minutes, headers are the same as in Table 2.

| Scenario | | Wait | I. Veh. | Walk | P. Trf. | Early | % Early | Late | % Late | % Inv. |
|---|---|---|---|---|---|---|---|---|---|---|
| T1 | Opt. | 10.9 | 32.1 | 1.0 | 7.2 | – | – | 8.0 | 57.3 | 18.2 |
| T2 | Opt. | 11.5 | 32.2 | 2.0 | 8.8 | – | – | 8.2 | 59.1 | 18.2 |
| T4 | Opt. | 12.6 | 32.4 | 4.0 | 11.5 | – | – | 8.3 | 65.5 | 18.2 |
| T8 | Opt. | 11.8 | 31.4 | 8.0 | 14.8 | – | – | 7.0 | 76.4 | 6.4 |

**Table 4**
Performance for each VI.

| Sc. | Baseline | | VI-1 | | | VI-2 | | | VI-3 | | | VI-4 | | | VI-5 | | |
|---|---|---|---|---|---|---|---|---|---|---|---|---|---|---|---|---|---|
| | CPU | Gap | CPU | Diff. | Gap | CPU | Diff. | Gap | CPU | Diff. | Gap | CPU | Diff. | Gap | CPU | Diff. | Gap |
| S1 | . | 6.18 | . | . | 9.5 | 4018 | -44.2 | - | . | . | 8.4 | . | . | 6.4 | . | . | 6.0 |
| S2 | . | 0.53 | 6685 | -7.2 | - | . | . | 0.2 | 6820 | -5.3 | – | 7192 | -0.1 | – | . | . | 0.8 |
| S3 | 3428 | – | 3042 | -11.2 | . - | 1515 | -55.8 | - | 3275 | -4.5 | – | 3540 | 3.3 | – | 3463 | 1.0 | – |
| S4 | 2724 | – | 3660 | 34.4 | – | 4210 | 54.6 | – | 2209 | -18.9 | - | 2818 | 3.5 | – | 2762 | 1.4 | – |
| S5 | 1694 | – | 1615 | -4.7 | – | 4045 | 138.7 | – | 1344 | -20.7 | - | 1617 | -4.5 | – | 1630 | -3.8 | – |
| S6 | 1459 | – | 1869 | 28.1 | – | 3156 | 116.4 | – | 1436 | -1.6 | - | 1455 | -0.2 | – | 1444 | -1.0 | – |
| S7 | 1113 | – | 1836 | 64.9 | – | 2139 | 92.1 | – | 1021 | -8.3 | - | 1108 | -0.5 | – | 1127 | 1.2 | – |
| S8 | 374 | – | 160 | -57.1 | - | 397 | 6.2 | – | 300 | -19.6 | – | 368 | -1.5 | – | 368 | -1.5 | – |
| Avg. | | | | 3.5 | | | 5.9 | | | -6.3 | | | 0.4 | – | | 0.0 | – |

Sc.: Scenario, Baseline: CPU time without VIs, CPU: CPU time in seconds, Diff.: Percentage difference of CPU time (%) compared to Baseline. Gap: Optimality gap (%). A period "." under the columns CPU and Diff. indicates that the scenario was not solved to optimality within two hours. The values in the final row are the average of the Diff. columns weighted by the Baseline CPU for each scenario. The weight for scenarios whose Baseline CPU is ".", is set to 7200. The best performing VI for each scenario is highlighted with gray background.

### *5.2.2. Performance of valid inequalities*

The performance of each individual valid inequality is presented in Table 4. For all scenarios, there exists at least one out of the five valid inequalities which reduces the computation time of the model. Notably for scenarios S1 and S2, the use of valid inequalities allows the problem to be solved to optimality within two hours, whereas without the addition of these valid inequalities, those scenarios cannot be solved to optimality within the same time. On average, VI-3 is the best among the five valid inequalities as it reduces computation time by an average of 6.3%. From the table, we can observe that for some scenarios that are easier to solve (based on the Baseline solve time), the use of some proposed valid inequalities have increased the solve time (e.g. VI-2 for S7). However, this is less significant when compared to the gains obtained from the use of the valid inequalities when solving

**Table 5**
Best-performing combinations of valid inequalities based on average percentage difference of solve time (%) across all scenarios (cuts added as regular constraints to the main model).

| Valid inequalities | S1 | S2 | S3 | S4 | S5 | S6 | S7 | S8 | Avg. |
|---|---|---|---|---|---|---|---|---|---|
| Baseline | . | . | 3428 | 2724 | 1694 | 1459 | 1113 | 374 | |
| 1 + 2 + 3 + 4 + 5 | -34.3 | -34.7 | -41.1 | **33.1** | -30.1 | **123.9** | **198.0** | -44.8 | -8.5 |
| 3 | . | -5.3 | -4.5 | -18.9 | -20.7 | -1.6 | -8.3 | -19.6 | -6.3 |
| 3 + 4 | . | -3.7 | -5.3 | -20.1 | -18.9 | -5.4 | -11.0 | -18.5 | -6.3 |
| 3 + 4 + 5 | . | -5.4 | -2.4 | -18.8 | -21.8 | -1.3 | -9.4 | -20.6 | -6.2 |
| 3 + 5 | . | -3.2 | -4.7 | -17.0 | -20.7 | -0.9 | -9.1 | -18.8 | -5.5 |
| 1 + 2 + 5 | . | -44.2 | -50.2 | **24.9** | -32.2 | **131.8** | **153.1** | -47.1 | -5.2 |
| 1 + 2 + 3 | . | -40.4 | -51.4 | **17.9** | -32.8 | **127.9** | **188.6** | -45.5 | -3.8 |
| 1 + 2 + 4 + 5 | . | -42.0 | -43.5 | **22.0** | -34.9 | **139.2** | **152.0** | -48.8 | -3.8 |
| 1 + 2 + 3 + 4 | . | -39.8 | -51.1 | **24.0** | -34.0 | **127.6** | **195.4** | -44.4 | -2.6 |
| 2 + 5 | -44.9 | . | -54.0 | **53.0** | **14.2** | **116.9** | **99.3** | **4.9** | -2.3 |

The values are given in percentage point units except in the first row where the Baseline CPU time is given in time units (seconds). A period "." indicates that the scenario was not solved to optimality within two hours. The final column is the average value across all scenarios weighted by their respective Baseline CPU time. The weights for scenarios whose Baseline CPU is ".", are set to 7200. The cases where the addition of VIs worsens the performance are highlighted in **bold**. The best-performing combination of VIs for each scenario is highlighted with gray background.

harder scenarios, as evident in scenarios S1, S2 and S3. This, however, suggests that the performance of each valid inequality is very much dependent on the problem that is being solved. It is also worth noting that while VI-4 and VI-5 have been proven to be useful in solving the timetable synchronization problem (Fouilhoux et al., 2016), the benefits of these valid inequalities seem to be insignificant when used to solve the problem presented in this study, which uses time-dependent travel time data.

In Table 5, the results obtained from the use of different combinations of valid inequalities are presented. The table lists the top ten best-performing combinations out of all possible combinations of the five valid inequalities. The combinations are evaluated and sorted based on of the weighted average of percentage solve time difference across all scenarios. Similar trends are observed for both scenarios S6 and S7, where the baseline solve time is generally lower than that with valid inequalities. However, the benefits of using these valid inequalities should instead be evaluated based on the more difficult scenarios. For instance, we can observe significantly larger gains with scenario S3 using a combination of valid inequalities. Although the performance of valid inequalities when used individually were unsatisfactory as presented in Table 4, they proved to be beneficial when used in tandem with the other valid inequalities.

#### *5.2.3. Implementing valid inequalities in a branch-and-cut framework*

In the previous section, the valid inequalities (VIs) are implemented as regular constraints in the mixed integer linear program given by (2) to (29), which results in large models. In this section, we employ the VIs derived in Section 4 within a branch-and-cut framework in an attempt to reduce the model size and increase computational efficiency.

At each node of the branch-and-cut tree, the LP relaxation of the current model is solved. The solution is then used to identify constraints that are violated, among the pool of valid inequalities. The violated constraints are added to the current model, and the relaxation of the resulting model is solved. In the solution process, the identification of violated constraints and the addition of those constraints to the model is repeated until all of the VIs are satisfied. The branch-and-cut algorithm then proceeds as usual. By doing so, the model size of the earlier stages of the optimization process remains small, thus resulting in less expensive computation of the LP relaxation. This strategy can be implemented easily by adding the VIs as user cuts in CPLEX.

The comparison between two strategies for the implementation of VIs are presented in Table 6. By comparing the performance of the individual classes of the VIs, one can observe that adding VI-1 and VI-4 as user cuts tend to reduce the solution time across most instances, whereas VI-2, VI-3 and VI-5 perform better when they are added as regular constraints in the original model. Generally speaking, the improvements from the addition of the VIs as user cuts are negligible at best, in most cases. In cases where the user cuts strategy is superior, the improvements are rather insignificant.

For the top ten best-performing combinations of the VIs, the observations are rather mixed. The maximum reduction in performance from adding the VIs as user cuts is 11.2% (VI-1 + VI-2 + VI-5 for S6) while the biggest improvement is observed at 11.3% (VI-1 + VI-2 + VI-3 + VI-4 for S7). However, these observations are rather rare and can very much be considered as outliers. In most cases, the performances do not vary much whether the valid inequalities are implemented one way or another. The results also seem to suggest that it is very dependent on the problem being solved, and the valid inequalities concerned.

## 6. Conclusion

In this study, we have developed a mixed integer linear programming (MILP) model for the PT schedule synchronization problem using time-dependent travel time data. It determines the timetable for the PT lines with the objective of improving the passengers' overall travel experience. Three valid inequalities (VIs) are derived for the MILP model by investigating the properties of the problem and two valid inequalities are developed by adapting the VIs in existing literature. The case study on a small network

**Table 6**
Performance of both cut implementation strategies across all scenarios.

| Valid inequalities | S1 | S2 | S3 | S4 | S5 | S6 | S7 | S8 | Avg. |
|---|---|---|---|---|---|---|---|---|---|
| Individual cuts | | | | | | | | | |
| 1 | . | −1.6 | **1.5** | −2.3 | **0.8** | **5.4** | −3.1 | −0.1 | −0.3 |
| 2 | −2.6 | . | **0.2** | **1.4** | **8.2** | **7.0** | −0.9 | **5.6** | **0.5** |
| 3 | . | **1.3** | **2.3** | **2.4** | **1.2** | −0.2 | **0.4** | **4.0** | **1.1** |
| 4 | . | . | −3.9 | −2.7 | **6.4** | −3.9 | **0.3** | **6.7** | −0.4 |
| 5 | . | . | **3.0** | **1.7** | −2.8 | −2.0 | **4.0** | **3.0** | **0.5** |
| Top 10 best-performing cuts | | | | | | | | | |
| 1 + 2 + 3 + 4 + 5 | **3.0** | −0.3 | −1.3 | −3.8 | −5.5 | −3.3 | −1.5 | −1.0 | −0.5 |
| 3 | . | **1.3** | **2.3** | **2.4** | **1.2** | −0.2 | **0.4** | **4.0** | **1.1** |
| 3 + 4 | . | . | **1.5** | **3.2** | −1.0 | **4.2** | **1.4** | **1.0** | **1.9** |
| 3 + 4 + 5 | . | . | −0.5 | −2.1 | **2.2** | −2.3 | −2.2 | **0.5** | **1.2** |
| 3 + 5 | . | **0.4** | **1.4** | **0.9** | −0.8 | **3.6** | −1.9 | **2.3** | **0.5** |
| 1 + 2 + 5 | . | **3.5** | −2.3 | **0.2** | −2.7 | **11.2** | **1.0** | **0.6** | **1.2** |
| 1 + 2 + 3 | . | **3.0** | **1.4** | **4.5** | −2.6 | −1.6 | −5.7 | **1.5** | **1.1** |
| 1 + 2 + 4 + 5 | . | **0.8** | −0.1 | **1.2** | −0.9 | −10.7 | −3.0 | **2.8** | −0.5 |
| 1 + 2 + 3 + 4 | . | **0.7** | **1.3** | **9.1** | −1.9 | −9.2 | −11.3 | −1.4 | **0.1** |
| 2 + 5 | **1.2** | . | **0.6** | −2.1 | **2.4** | **4.0** | **2.3** | **7.3** | **0.9** |

The values are given by (as in Tables 4 and 5) are the percentage difference of solve time for respective implementation. Negative values indicate that adding the valid inequalities as user cuts reduces solve time and vice versa. A period "." indicates that no improvement is observed, whether because both implementations result in the same solve time, or neither implementation results in the scenarios being solved to optimality within two hours. The cases where the addition of VIs as user cuts worsens the performance are highlighted in **bold**.

shows that using time-dependent travel time data could reduce passengers' transfer time, as well as other time-related attributes that contribute towards a passenger's travel experience. The performance of the VIs is examined using a network of three main bus lines in Copenhagen. The results show that the use of time-dependent travel time data can significantly reduce the time-related attributes and improve passengers' overall travel experience. We observed an average reduction of about 78% for waiting time at origin and path transfer time, whereas in-vehicle time and late arrivals are down by 13.4% and 33.3 percentage points respectively. The number of trips that cannot be completed due to missed connections is also significantly reduced. On the other hand, we also show that using either one VI or a combination of different VIs could significantly reduce the computation time. The maximum reduction in solve time is higher than 50% in certain scenarios, and the average reduction is 8.5%. We also show that by adding the VIs gradually as we go deeper in the branch-and-cut tree, we can further improve the performance in some cases, depending on the scenario and valid inequalities used.

From a practitioner's perspective, there are a few points to consider when applying the developed method on a real-size transit network. These points are added to the practical consideration, in the modeling, of using time-dependent travel time data in the synchronization of schedules. The number of variables and constraints of our model scales linearly with the number of possible transfers in the network, and exponentially with the number of trips considered within the planning horizon. Thus, we recommend that the daily operational time span be split into multiple smaller and more reasonable planning horizon to curb the exponential growth in model complexity. This split should be carried out with the minimization of the number of trips that start and end within different planning horizon because the time-related attributes for these trips cannot be accurately quantified. Our formulation could be suitable for both schedule and headway-based systems, though the optimized schedules would be schedule-based. The practical network parameters considered as an input to the model are mainly associated with the level of service, e.g., the number of trips within a planning horizon and the allowable headway range, which can be quantified for both schedule and headway-based systems.

Finally, this work opens the door to various research directions for future PT scheduling research using big data, as follows:

1. A straightforward extension would be to strengthen the VIs or to explore whether, or not, there are other VIs while realizing that the performance of the VIs varies. Practically speaking, this involves deriving a VI or a combination of VIs having a robust performance.
2. This study considers does not explicitly consider the different types of transfer stations and their respective characteristics as in Hadas and Ranjitkar (2012). In our model, we internalized the characteristics of the stops within a single parameter $W_{rr's}$. Thus in future studies, one possible avenue for an extension will be to differentiate the different types of transfer stations explicitly within the model.
3. The objective function considered is only with time-related attributes, thus a more general connectivity measure that captures other qualitative and quantitative attributes, as established by Ceder (2016), warrants consideration.
4. This study assumes that the time dependent travel time data used is given and is deterministic for practical reasons. Travel time, however, is inherently stochastic as it is affected by many factors that are within and outside the control of a transit planner. Therefore, a possible direction will be to consider the uncertainties of the time-dependent travel time data and develop robust optimization models for solving the problem.
5. This study utilizes only time-dependent travel time data, but possible adjustments of timetables and application of different control mechanisms can also affect the time-dependent travel demand (Wu et al., 2016). Thus, it is possible to develop a bilevel modeling framework (Szeto and Jiang, 2014; Zhao et al., 2018) to capture the interaction between supply and demand

by embedding a transit assignment model (Hamdouch et al., 2014; Parbo et al., 2014; Jiang and Szeto, 2016; Wu et al., 2019; Xie et al., 2020; Jiang and Ceder, 2021; Xie et al., 2021; Jiang, 2021).

6. For the ease of developing VIs, this study simplifies the computation of the dwell time, which, in reality, is affected by the process and behavior of passengers' boarding and alighting. Incorporating it into the VIs would not be trivial and require significant future research efforts.
7. Following the aforementioned Item 5 and Item 6 it is expected that a realistic transit assignment model with time-dependent demand and passenger motion, would yield a considerable computation burden. Some possible solutions would be the use of metamodeling, statistical learning, or machine learning approaches, such as that described by Song et al. (2018) and Fusco et al. (2015).

## CRediT authorship contribution statement

**Kelvin Lee:** Conceptualization, Methodology, Software, Validation, Formal analysis, Writing – original draft, Writing – review & editing, Visualization. **Yu Jiang:** Conceptualization, Methodology, Validation, Writing – original draft, Writing – review & editing, Supervision. **Avishai (Avi) Ceder:** Writing – review & editing, Supervision. **Justin Dauwels:** Resources, Supervision. **Rong Su:** Resources, Supervision. **Otto Anker Nielsen:** Resources, Funding acquisition, Supervision.

## Acknowledgments

The authors would like to thank the editor and three anonymous referees for their valuable and constructive comments. This research is partially supported by A*STAR under its RIE2020 Advanced Manufacturing and Engineering (AME) Industry Alignment Fund Pre Positioning (IAF-PP) (Award A19D6a0053), National Natural Science Foundation of China (71971038). The computational work for this article was partially performed on resources of the National Supercomputing Centre, Singapore.

The paper was accepted for presentation at the 15th CASPT international conference (CASPT2021) about Public Transport, organized by Dr. Yuval Hadas, Prof. Avi Ceder and Prof. Oded Cats.

## Appendix A. Proof for Eq. (VI-1)

Given the departure time of the $(k'+1)$th vehicle of transit line $r'$ and the maximum and minimum allowable headway for transit line $r'$, we can write the lower and upper bounds for the departure of the $k'$th vehicle of transit line $r'$ as follows:

$$d_{r's}^{k'+1} - \overline{H}_{r'} \le d_{r's}^{k'} \le d_{r's}^{k'+1} - \underline{H}_{r'} \tag{A.1}$$

and by using the same inequalities for $d_{r's}^{k'+1}$, we have the following:

$$d_{r's}^{k'+2} - 2\overline{H}_{r'} \le d_{r's}^{k'+1} - \overline{H}_{r'} \le d_{r's}^{k'} \le d_{r's}^{k'+1} - \underline{H}_{r'} \le d_{r's}^{k'+2} - 2\underline{H}_{r'} \tag{A.2}$$

Then by induction we have the following relationship:

$$d_{r's}^{|K_{r'}|} - \left(|K_{r'}| - k'\right)\overline{H}_{r'} \le d_{r's}^{k'} \le d_{r's}^{|K_{r'}|} - \left(|K_{r'}| - k'\right)\underline{H}_{r'} \tag{A.3}$$

By definition, when the transfer from the $k$th vehicle of transit line $r$ to $k'$th vehicle of transit line $r'$ is feasible, i.e. $\Delta_{rr's}^{kk'} = 1$, all subsequent transfers to the $i$th vehicle of transit line $r'$, where $i > k'$, are also feasible. Therefore, we can write the following:

$$\Delta_{rr's}^{kk'} = 1 \implies \sum_{i=k'}^{|K_{r'}|} \Delta_{rr's}^{ki} - 1 = |K_{r'}| - k' \tag{A.4}$$

Using this definition, we can rewrite (A.3) in terms of the transfer feasibility variables as such:

$$d_{r's}^{|K_{r'}|} - \left(\sum_{i=k'}^{|K_{r'}|} \Delta_{rr's}^{ki} - 1\right)\overline{H}_{r'} \le d_{r's}^{k'} \le d_{r's}^{|K_{r'}|} - \left(\sum_{i=k'}^{|K_{r'}|} \Delta_{rr's}^{ki} - 1\right)\underline{H}_{r'} \tag{A.5}$$

Note, however, that the inequalities above are only valid when $\Delta_{rr's}^{kk'} = 1$ (see Fig. A.7(b)). When $\Delta_{rr's}^{kk'} = 0$, the summation would be equivalent to a summation that starts from $i = i'$, where the $i'$th vehicle is the first vehicle of transit line $r'$ such that the transfer from the $k$th vehicle of transit line $r$ is possible (see Fig. A.7(a)). Hence, instead of giving the feasible range for $d_{r's}^{k'}$, the left-hand side and right-hand-side terms of (A.5) gives the feasible range for the departure of the first bus for which the transfer from transit line $r$ to transit line $r'$.

The inequalities in (VI-1) indicate that when $\Delta_{rr's}^{kk'} = 0$, the following expression must hold:

$$d_{r's}^{|K_{r'}|} - \sum_{i=k'}^{|K_{r'}|} \Delta_{rr's}^{ki}\overline{H}_{r'} < a_{rs}^{k} + W_{rr's} \tag{A.6}$$

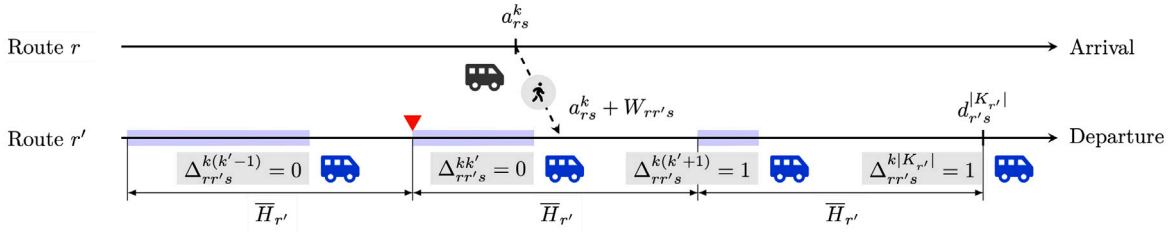


(a) When $\Delta^{kk'}_{rr's} = 0$, then $d^{|K_{r'}|}_{r's} - \sum_{i=k'}^{|K_{r'}|} \Delta^{ki}_{rr's}\overline{H}_r$ gives the earliest allowable departure of the first trip of route $r'$ where transfer from the $k$th vehicle of transit line $r$ is possible (indicated by the red triangle). In this case, Eq. (VI-1) indicates that $d^{|K_{r'}|}_{r's} - \sum_{i-k'}^{|K_{r'}|} \Delta^{ki}_{rr's}\overline{H}_r - a^k_{rs} - W_{rr's} < 0$.

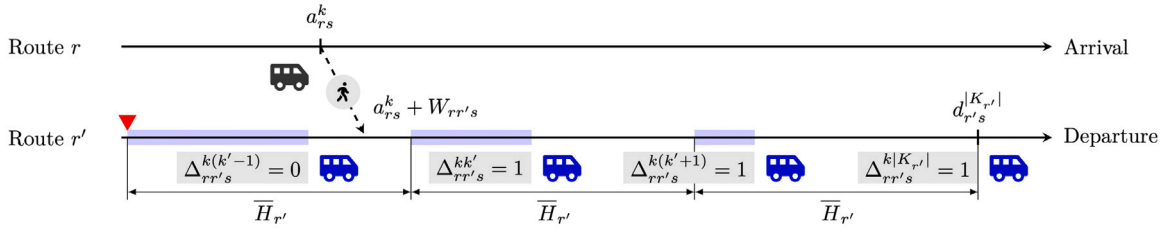


(b) When $\Delta^{kk'}_{rr's} = 1$, then $d^{|K_{r'}|}_{r's} - \sum_{i=k'}^{|K_{r'}|} \Delta^{ki}_{rr's}\overline{H}_r$ gives the earliest allowable departure of the previous trip $k'-1$ (indicated by the red triangle). In this case, Eq. (VI-1) indicates that $d^{|K_{r'}|}_{r's} - \sum_{i-k'}^{|K_{r'}|} \Delta^{ki}_{rr's}\overline{H}_r - a^k_{rs} - W_{rr's} \geq 0$.

**Fig. A.7.** Illustration of Eq. (VI-1) for different possibilities of $\Delta^{kk'}_{rr's}$. The figure shows the arrival and departure times of trips on transit lines $r$ and $r'$ on time axes, where the shaded bars indicate the range of allowable departure times of each trip on transit line $r'$ based on the allowable headway range.

Since $\Delta^{kk'}_{rr's} = 0$, the terms on the left hand side of (A.6) gives the earliest departure of the vehicle that comes before the first vehicle of transit line $r'$ to which the transfer from the $k$th vehicle of transit line $r$ is possible. To put it in mathematical terms:

$$\Delta^{kk'}_{rr's} = 0 \implies d^{|K_{r'}|}_{r's} - \sum_{i=k'}^{|K_{r'}|} \Delta^{ki}_{rr's}\overline{H}_{r'} = \min(d^{j-1}_{r's}) \quad \text{such that } j > k', \Delta^{k(j-1)}_{rr's} = 0, \Delta^{kj}_{rr's} = 1 \tag{A.7}$$

Hence, when $\Delta^{kk'}_{rr's} = 0$, the expression in (A.6) holds since, by definition, the transfer to the $(j-1)$th vehicle of transit line $r'$ is not possible implies that the departure of the vehicle has to be earlier than $a^k_{rs} + W_{rr's}$.

On the other hand, when the left-hand side of (VI-1) is no less than zero, $\Delta^{kk'}_{rr's} = 1$. This can be proven by contradiction. Suppose that the left-hand side is greater than zero, and $\Delta^{kk'}_{rr's} = 0$, the left-hand side becomes $\min(d^{j-1}_{r's}) \geq a^k_{rs} + W_{rr's}$ where $j$ is as defined in (A.7). This is clearly a contradiction, since, by definition, $\min(d^{j-1}_{r's}) < a^k_{rs} + W_{rr's}$. Hence, the inequality in (VI-1) is valid. □

## Appendix B. Proof for Eq. (VI-2)

When $\delta^{kk'}_{grr's} = 1$, passenger group $g$ will not be able to make the transfer from the $k$th vehicle of transit line $r$ to the $(k'-1)$th vehicle of transit line $r'$, i.e. $\delta^{k(k'-1)}_{grr's} = 0$, because it is assumed that the passengers always board the earliest possible vehicle of the connecting route. Hence the arrival time of the passengers at the platform for route $r'$ at station $s$, i.e. $a^k_{rs} + W_{rr's}$ has to be later than the departure time of the $(k'-1)$th bus of the connecting route $r'$. Mathematically, it can be written as follows:

$$a^k_{rs} + W_{rr's} > d^{k'-1}_{r's} \tag{B.1}$$

This can be proven by contradiction. Let $\delta^{kk'}_{grr's} = 1$ and $a^k_{rs} + W_{rr's} \leq d^{k'-1}_{r's}$ be true, then there exists $\dot{k} = k'-1 < k'$ such that $d^{\dot{k}}_{r's} < d^{k'}_{r's}$ and $a^k_{rs} + W_{rr's} \leq d^{\dot{k}}_{r's}$. By definition, the passengers would make the earliest possible transfer, which means that $\delta^{k\dot{k}}_{grr's} = 1$ and $\delta^{kk'}_{grr's} = 0$. This contradicts with the premise, hence proving inequality (B.1) true. Note, however, that the converse is not necessarily true.

When $\delta^{kk'}_{grr's} = 1$, $\Delta^{kk'}_{rr's} = 1$ must also be true, and hence we can rewrite inequality (B.1) as follows using the relationship given in (A.5):

$$a^k_{rs} + W_{rr's} > d^{k'-1}_{r's} \geq d^{\dot{k}'}_{r's} - \sum_{i=k'}^{\dot{k}'} \Delta^{ki}_{rr's}\overline{H}_{r'} \qquad \forall (r, r', s) \in \Psi \quad k \in K_r \quad k', \dot{k}' \in K_{r'} \quad \dot{k}' \geq k' \tag{B.2}$$

By rearranging and collecting the terms on the left-hand side, we have:

$$a^k_{rs} + W_{rr's} - d^{k'}_{r's} + \sum_{i=k'}^{\dot{k}'} \Delta^{ki}_{rr's} \overline{H}_{r'} > 0 \qquad \forall (r,r',s) \in \Psi \quad k \in K_r \quad k', \dot{k}' \in K_{r'} \quad \dot{k}' \geq k' \text{ (B.3)}$$

Since the inequality above is true when $\delta^{kk'}_{grr's} = 1$, we can write it as follows:

$$a^k_{rs} + W_{rr's} - d^{\dot{k}'}_{r's} + \sum_{i=k'}^{\dot{k}'} \Delta^{ki}_{rr's} \overline{H}_{r'} > M(\delta^{kk'}_{grr's} - 1) \qquad \forall (r,r',s) \in \Psi \quad k \in K_r \quad k', \dot{k}' \in K_{r'} \quad \dot{k}' \geq k' \text{ (B.4)}$$

Similarly, if the earliest departure of $(k'-1)$th vehicle of transit line $r'$ from station $s$ is later than $a^k_{rs} + W_{rr's} + \overline{P}_g$, where $\overline{P}_g$ is the maximum path transfer time, the transfer from the $k$th vehicle of transit line $r$ to the $(k'-1)$th vehicle of transit line $r'$ will not be possible, and therefore the transfer to $k'$th vehicle of transit line $r'$ will not be possible as well. Note, that the converse of this statement may not be true. We state as follows:

$$a^k_{rs} + W_{rr's} + \overline{P}_g < \min\left(d^{k'-1}_{r's}\right) \implies \delta^{k(k'-1)}_{grr's} = 0 \implies \delta^{kk'}_{grr's} = 0 \qquad \forall (r,r',s) \in \Psi \quad k \in K_r \quad k' \in K_{r'} \text{ (B.5)}$$

We can rewrite the earliest possible departure time term $\min\left(d^{k'-1}_{r's}\right)$ in inequality (B.5) using (A.5) as follows:

$$a^k_{rs} + W_{rr's} + \overline{P}_g < d^{k'}_{r's} - \sum_{i=k'}^{\dot{k}'} \Delta^{ki}_{rr's} \overline{H}_{r'} \qquad \forall (r,r',s) \in \Psi \quad k \in K_r \quad k', \dot{k}' \in K_{r'} \quad \dot{k}' \geq k' \text{ (B.6)}$$

By rearranging the terms, we have:

$$a^k_{rs} + W_{rr's} + \overline{P}_g - d^{\dot{k}'}_{r's} + \sum_{i=k'}^{\dot{k}'} \Delta^{ki}_{rr's} \overline{H}_{r'} < 0 \qquad \forall (r,r',s) \in \Psi \quad k \in K_r \quad k', \dot{k}' \in K_{r'} \quad \dot{k}' \geq k' \text{ (B.7)}$$

Since the inequality above is true when $\delta^{kk'}_{grr's} = 0$, we can write the following:

$$a^k_{rs} + W_{rr's} + \overline{P}_g - d^{\dot{k}'}_{r's} + \sum_{i=r'}^{k'} \Delta^{kk'}_{rr's} \overline{H}_{r'} > M\left(\delta^{kk'}_{grr's} - 1\right) \qquad \forall (r,r',s) \in \Psi \quad k \in K_r \quad k', \dot{k}' \in K_{r'} \quad \dot{k}' \geq k' \text{ (B.8)}$$

The inequalities in (B.4) and (B.8) can be combined to obtain the valid inequalities in Constraint (VI-2). □

## Appendix C. Proof for Eq. (VI-3)

The inequalities in Constraint (12) can be split into two inequalities:

$$\Delta^{kk'}_{rr's} = 0 \iff d^{k'}_{r's} < a^k_{rs} + W_{rr's} \qquad \forall (r,r',s) \in \Psi \quad k \in K_r \quad k' \in K_{r'} \text{ (C.1)}$$

$$\Delta^{kk'}_{rr's} = 1 \iff d^{k'}_{r's} \geq a^k_{rs} + W_{rr's} \qquad \forall (r,r',s) \in \Psi \quad k \in K_r \quad k' \in K_{r'} \text{ (C.2)}$$

The inequalities in (C.1) and (C.2) can be written in alternative form as given in (C.3) and (C.4), which gives Constraint (C.5) when they are combined.

$$\text{If } \Delta^{kk'}_{rr's} = 1 \implies \frac{d^{k'}_{r's} - a^k_{rs}}{W_{rr's}} \geq 1 \qquad \forall (r,r',s) \in \Psi \quad k \in K_r \quad k' \in K_{r'} \text{ (C.3)}$$

$$\text{If } \Delta^{kk'}_{rr's} = 0 \implies \frac{d^{k'}_{r's} - a^k_{rs}}{W_{rr's}} < 1 \qquad \forall (r,r',s) \in \Psi \quad k \in K_r \quad k' \in K_{r'} \text{ (C.4)}$$

$$\Delta^{kk'}_{rr's} \leq \max\left(0, \frac{d^{k'}_{r's} - a^k_{rs}}{W_{rr's}}\right) \qquad \forall (r,r',s) \in \Psi \quad k \in K_r \quad k' \in K_{r'} \text{ (C.5)}$$

By using Constraint (6) and Constraint (8), we can rewrite the arrival and departure times in terms of the departure time from the first station of the transit line, $d^k_{rs(1)}$, the departure time window decision variables, $\varphi^{k\tau}_{rs(i)}$, and the dwell time, $u^k_{rs(i)}$, at each station traversed by the transit line as follows:

$$\begin{aligned} d^k_{rs(i)} &= a^k_{rs(i)} + u^k_{rs(i)} \\ &= d^k_{rs(i-1)} + \sum_{\tau \in T} \varphi^{k\tau}_{rs(i-1)} t^{\tau}_{rs(i-1)} + u^k_{rs(i)} \end{aligned}$$

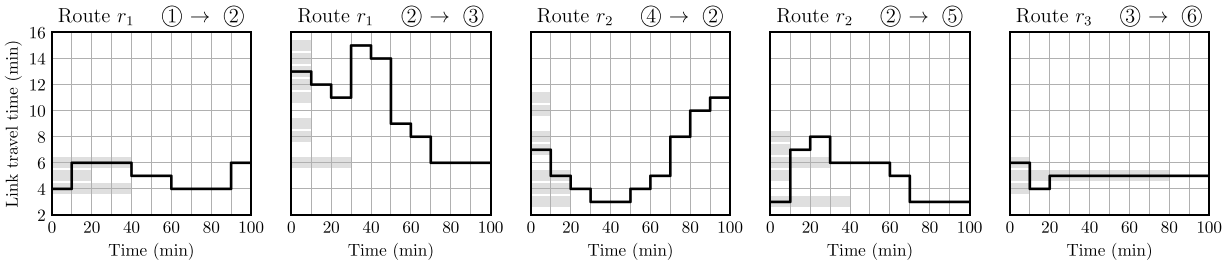


**Fig. D.8.** Time-dependent travel time of all links in the small artificial network. The bars on the $y$-axis shows the travel time distribution of each link. In this, the time interval for which the travel time data remains valid, i.e. $\vartheta$ is ten minutes.


**Fig. D.9.** An illustration of the optimized schedule versus the realized schedule for a bus on routes $r_1$ and $r2$ respectively.

$$= d^k_{rs_{(1)}} + \sum_{j=1}^{i} \sum_{\tau \in T} \varphi^{k\tau}_{rs_{(j)}} t^{\tau}_{rs_{(j)}} + \sum_{j=2}^{i} u^k_{rs_{(j)}}$$

$$= a^k_{rs_{(1)}} + \sum_{j=1}^{i} \sum_{\tau \in T} \varphi^{k\tau}_{rs_{(j)}} t^{\tau}_{rs_{(j)}} + \sum_{j=1}^{i} u^k_{rs_{(j)}} \tag{C.6}$$

$$a^k_{rs_{(i)}} = a^k_{rs_{(1)}} + \sum_{j=1}^{i} \sum_{\tau \in T} \varphi^{k\tau}_{rs_{(j)}} t^{\tau}_{rs_{(j)}} + \sum_{j=1}^{i-1} u^k_{rs_{(j)}} \tag{C.7}$$

Substituting Eqs. (C.6) and (C.7) into (C.5), we obtain the valid inequalities given in (VI-3). □

## Appendix D. Experimental setup and parameters for Section 5.1

In Section 5.1, we have generated a small artificial network of three routes and six nodes to illustrate the importance of considering time-independent travel time data in PT synchronization problems. We compared the itineraries of the three passenger groups subject to three different itineraries.

In Fig. 4(a), the passengers are subjected to a constant headway schedule. To obtain the constant headway schedule, we set the headway of each route to $\overline{D}/|K_r|$, and the departure time of the last bus of each route to $\overline{D}$. In this case, we use the mean travel time data $T_{rss'}$ to determine the arrival and departure times at each stop.

Once we obtain the constant headway schedule, we use it as a plan that is to be followed by the driver of each bus. We follow the entire trip of each bus from its origin to destination, and keep track of the true arrival and departure times of the trips with the true time-dependent travel time in Fig. D.8. Each bus tries to adhere to the optimized schedule as closely as possible, i.e. always depart on time from each stop. In the following exposition, we provide two examples in Fig. D.9 to demonstrate how we determine the realized arrival and departure times of each trip from the scheduled arrivals and departures.

For instance, in Fig. D.9(a) the bus is scheduled to depart from stop ① at $t = 5$ and arrive at stop ② at $t = 10$ as the mean travel time between the two stops is five minutes. However, the true travel time between the two nodes is four minutes at the time of departure as can be observed in the time-dependent travel time data (see Fig. D.8). Thus the bus shall arrive at stop ② at $t = 9$. Although the bus is scheduled to stop at ② for only one minute before departing at $t = 11$, the bus will instead stop for two minutes before departing at the scheduled departure time of $t = 11$. Once the realized arrival and departure times are determined, we follow the passengers from their origin and destinations using the realized times to obtain the passengers' itineraries as presented in Fig. 4(a).

For Fig. 4(b), we solve the optimization presented in Section 3 to obtain the schedules using mean travel time data $T_{rss'}$. The mean travel time data is obtained by taking the average value of the travel time curves in Fig. D.8. We do so to simulate the situation when time-dependent travel time data is not available, in which case an approximate mean historical travel time is used. This is often the case in real-world transit planning and scheduling. Once we have optimized schedule, we repeat the procedures as before to obtain the realized arrival and departure times and to determine the passengers itineraries in Fig. 4(b). We do the same for Fig. 4(c), albeit with time-dependent travel time, instead of the mean travel time.

**Table D.7**
Parameters used for the experiments in Section 5.1.

| Parameter | Value | Description |
|---|---|---|
| $\left[\underline{H}_r, \overline{H}_r\right]$ | [5, 30] | Allowable headway range |
| $\left[\underline{U}_{rs}, \overline{U}_{rs}\right]$ | [1, 2] | Allowable dwell time range |
| $\vartheta$ | 10 | Time interval for which time-dependent travel time remains constant |
| $\overline{P}_g$ | 20 | Maximum path transfer time |
| $\overline{D}$ | 40 | Planning horizon |
| $C_w$ | 1.5 | Time value of for waiting time |
| $C_v$ | 1 | Time value of in-vehicle time |
| $C_p$ | 1.5 | Time value for transfer time |
| $C_e$ | 0.5 | Penalty for early arrivals |
| $C_l$ | 2 | Penalty for late arrivals |

**Table E.8**
Parameters used for the experiments in Section 5.2. Parameters whose value is different to that in Table D.7 are highlighted in **bold**.

| Parameter | Value | Description |
|---|---|---|
| $\left[\underline{H}_r, \overline{H}_r\right]$ | [5, 30] | Allowable headway range |
| $\left[\underline{U}_{rs}, \overline{U}_{rs}\right]$ | [1, 2] | Allowable dwell time range |
| $\vartheta$ | **15** | Time interval for which time-dependent travel time remains constant |
| $\overline{P}_g$ | 20 | Maximum path transfer time |
| $\overline{D}$ | **60** | Planning horizon |
| $C_w$ | 1.5 | Time value of for waiting time |
| $C_v$ | 1 | Time value of in-vehicle time |
| $C_p$ | 1.5 | Time value for transfer time |
| $C_e$ | 0.5 | Penalty for early arrivals |
| $C_l$ | 2 | Penalty for late arrivals |

The parameters used when optimizing the schedules for Section 5.1 are given in Table D.7.

## Appendix E. Experimental setup and parameters for Section 5.2

The experimental setup used in Section 5.2 are mostly similar to that in Section 5.1 except for a few parameters. In particular, we used the same method to determine the constant headway and optimized schedules, realized arrival and departure times, and passengers' itineraries for Table 2. The parameters used in Section 5.2 are given in Table E.8 and the scenarios generated can be accessed at https://github.com/leeke2/tt-sync-scenarios.

## References


Abdolmaleki, M., Masoud, N., Yin, Y., 2020. Transit timetable synchronization for transfer time minimization. Transp. Res. B 131, 143–159. http://dx.doi.org/10.1016/j.trb.2019.12.002.

Allen, J., Muñoz, J.C., Rosell, J., 2019. Effect of a major network reform on bus transit satisfaction. Transp. Res. A 124, 310–333. http://dx.doi.org/10.1016/j.tra.2019.04.002.

Badia, H., Argote-Cabanero, J., Daganzo, C.F., 2017. How network structure can boost and shape the demand for bus transit. Transp. Res. A 103, 83–94. http://dx.doi.org/10.1016/j.tra.2017.05.030.

Beirão, G., Sarsfield Cabral, J.A., 2007. Understanding attitudes towards public transport and private car: A qualitative study. Transp. Policy 14, 478–489. http://dx.doi.org/10.1016/j.tranpol.2007.04.009.

Bookbinder, J.H., Désilets, A., 1992. Transfer optimization in a transit network. Transp. Sci. 26, 106–118. http://dx.doi.org/10.1287/trsc.26.2.106.

Ceder, A., 2016. Public Transit Planning and Operation: Modeling, Practice and Behavior, second ed. CRC Press, http://dx.doi.org/10.1201/b18689.

Ceder, A.A., 2021. Syncing sustainable urban mobility with public transit policy trends based on global data analysis. Sci. Rep. 11, 14597. http://dx.doi.org/10.1038/s41598-021-93741-4.

Ceder, A., Golany, B., Tal, O., 2001. Creating bus timetables with maximal synchronization. Transp. Res. A 35, 913–928. http://dx.doi.org/10.1016/S0965-8564(00)00032-X.

Ceder, A.a., Hassold, S., Dano, B., 2013. Approaching even-load and even-headway transit timetables using different bus sizes. Public Transport 5, 193–217. http://dx.doi.org/10.1007/s12469-013-0062-z.

Ceder, A., Tal, O., 2001. Designing synchronization into bus timetables. Transp. Res. Rec. J. Transp. Res. Board 1760, 28–33. http://dx.doi.org/10.3141/1760-04.

Ceder, A.a., Teh, C.S.c., 2010. Comparing public transport connectivity measures of major New Zealand cities. Transp. Res. Rec. J. Transp. Res. Board 2143, 24–33. http://dx.doi.org/10.3141/2143-04.

Chakrabarti, S., 2017. How can public transit get people out of their cars? An analysis of transit mode choice for commute trips in Los Angeles. Transp. Policy 54, 80–89. http://dx.doi.org/10.1016/j.tranpol.2016.11.005.

Dessouky, M., Hall, R., Zhang, L., Singh, A., 2003. Real-time control of buses for schedule coordination at a terminal. Transp. Res. A 37, 145–164. http://dx.doi.org/10.1016/S0965-8564(02)00010-1.

Fouilhoux, P., Ibarra-Rojas, O.J., Kedad-Sidhoum, S., Rios-Solis, Y.A., 2016. Valid inequalities for the synchronization bus timetabling problem. European J. Oper. Res. 251, 442–450. http://dx.doi.org/10.1016/j.ejor.2015.12.006.

Fusco, G., Colombaroni, C., Comelli, L., Isaenko, N., 2015. Short-term traffic predictions on large urban traffic networks: Applications of network-based machine learning models and dynamic traffic assignment models. In: 2015 International Conference on Models and Technologies for Intelligent Transportation Systems. MT-ITS, pp. 93–101. http://dx.doi.org/10.1109/MTITS.2015.7223242.

Guo, Z., Wilson, N.H.M., 2011. Assessing the cost of transfer inconvenience in public transport systems: A case study of the London underground. Transp. Res. A 45, 91–104. http://dx.doi.org/10.1016/j.tra.2010.11.002.

Hadas, Y., Ranjitkar, P., 2012. Modeling public-transit connectivity with spatial quality-of-transfer measurements. J. Transp. Geogr. 22, 137–147. http://dx.doi.org/10.1016/j.jtrangeo.2011.12.003.

Hall, R.W., 1986. The fastest path through a network with random time-dependent travel times. Transp. Sci. 20, 182–188. http://dx.doi.org/10.1287/trsc.20.3.182.

Hamdouch, Y., Szeto, W.Y., Jiang, Y., 2014. A new schedule-based transit assignment model with travel strategies and supply uncertainties. Transp. Res. B 67, 35–67. http://dx.doi.org/10.1016/j.trb.2014.05.002.

Hine, J., Scott, J., 2000. Seamless, accessible travel: Users' views of the public transport journey and interchange. Transp. Policy 7, 217–226. http://dx.doi.org/10.1016/S0967-070X(00)00022-6.

Ibarra-Rojas, O.J., Delgado, F., Giesen, R., Muñoz, J.C., 2015. Planning, operation, and control of bus transport systems: A literature review. Transp. Res. B 77, 38–75. http://dx.doi.org/10.1016/j.trb.2015.03.002.

Ibarra-Rojas, O.J., Rios-Solis, Y.A., 2012. Synchronization of bus timetabling. Transp. Res. B 46, 599–614. http://dx.doi.org/10.1016/j.trb.2012.01.006.

Ichoua, S., Gendreau, M., Potvin, J.-Y., 2003. Vehicle dispatching with time-dependent travel times. European J. Oper. Res. 144, 379–396. http://dx.doi.org/10.1016/S0377-2217(02)00147-9.

Jiang, Y., 2021. Reliability-based equitable transit frequency design. Transportmetrica A 1–31. http://dx.doi.org/10.1080/23249935.2021.1902420.

Jiang, Y., Ceder, A.a., 2021. Incorporating personalization and bounded rationality into stochastic transit assignment model. Transp. Res. C 127, 103127. http://dx.doi.org/10.1016/j.trc.2021.103127.

Jiang, Y., Szeto, W.Y., 2016. Reliability-based stochastic transit assignment: Formulations and capacity paradox. Transp. Res. B 93, 181–206. http://dx.doi.org/10.1016/j.trb.2016.06.008.

Klemt, W.-D., Stemme, W., 1988. Schedule synchronization for public transit networks. In: Computer-Aided Transit Scheduling. Springer, Berlin Heidelberg, pp. 327–335. http://dx.doi.org/10.1007/978-3-642-85966-3_28.

Liu, R., Li, S., Yang, L., Yin, J., 2020. Energy-efficient subway train scheduling design with time-dependent demand based on an approximate dynamic programming approach. IEEE Trans. Syst. Man Cybern. 50, 2475–2490. http://dx.doi.org/10.1109/TSMC.2018.2818263.

Liu, L., Miller, H.J., 2020. Measuring risk of missing transfers in public transit systems using high-resolution schedule and real-time bus location data. Urban Stud. 0042098020919323. http://dx.doi.org/10.1177/0042098020919323.

Malandraki, C., Daskin, M.S., 1992. Time dependent vehicle routing problems: Formulations, properties and heuristic algorithms. Transp. Sci. 26, 185–200. http://dx.doi.org/10.1287/trsc.26.3.185.

Menon, A.K., Lee, Y., 2017. Predicting short-term public transport demand via inhomogeneous Poisson processes. In: Proceedings of the 2017 ACM on Conference on Information and Knowledge Management. CIKM '17, Association for Computing Machinery, New York, NY, USA, pp. 2207–2210. http://dx.doi.org/10.1145/3132847.3133058.

Milan, B.F., Creutzig, F., 2017. Lifting peripheral fortunes: Upgrading transit improves spatial, income and gender equity in medellin. Cities 70, 122–134. http://dx.doi.org/10.1016/j.cities.2017.07.019.

Niu, H., Zhou, X., 2013. Optimizing urban rail timetable under time-dependent demand and oversaturated conditions. Transp. Res. C 36, 212–230. http://dx.doi.org/10.1016/j.trc.2013.08.016.

Niu, H., Zhou, X., Gao, R., 2015. Train scheduling for minimizing passenger waiting time with time-dependent demand and skip-stop patterns: Nonlinear integer programming models with linear constraints. Transp. Res. B 76, 117–135. http://dx.doi.org/10.1016/j.trb.2015.03.004.

Nuzzolo, A., Crisalli, U., 2004. The schedule-based approach in dynamic transit modelling: A general overview. In: Wilson, N.H.M., Nuzzolo, A. (Eds.), Schedule-Based Dynamic Transit Modeling: Theory and Applications. Springer US, Boston, MA, pp. 1–24. http://dx.doi.org/10.1007/978-1-4757-6467-3_1.

Nuzzolo, A., Russo, F., Crisalli, U., 2001. A doubly dynamic schedule-based assignment model for transit networks. Transp. Sci. 35, 268–285. http://dx.doi.org/10.1287/trsc.35.3.268.10149.

van Oort, N., Brands, T., de Romph, E., 2015. Short-term prediction of ridership on public transport with smart card data. Transp. Res. Rec. J. Transp. Res. Board 2535, 105–111. http://dx.doi.org/10.3141/2535-12.

O'Sullivan, A., Pereira, F.C., Zhao, J., Koutsopoulos, H.N., 2016. Uncertainty in bus arrival time predictions: Treating heteroscedasticity with a metamodel approach. IEEE Trans. Intell. Trans. Syst. 17, 3286–3296. http://dx.doi.org/10.1109/TITS.2016.2547184.

Pang, J., Huang, J., Du, Y., Yu, H., Huang, Q., Yin, B., 2019. Learning to predict bus arrival time from heterogeneous measurements via recurrent neural network. IEEE Trans. Intell. Trans. Syst. 20, 3283–3293. http://dx.doi.org/10.1109/TITS.2018.2873747.

Parbo, J., Nielsen, O.A., Prato, C.G., 2014. User perspectives in public transport timetable optimisation. Transp. Res. C 48, 269–284. http://dx.doi.org/10.1016/j.trc.2014.09.005.

Petersen, N.C., Rodrigues, F., Pereira, F.C., 2019. Multi-output bus travel time prediction with convolutional LSTM neural network. Expert Syst. Appl. 120, 426–435. http://dx.doi.org/10.1016/j.eswa.2018.11.028.

Poon, M.H., Wong, S.C., Tong, C.O., 2004. A dynamic schedule-based model for congested transit networks. Transp. Res. B 38, 343–368. http://dx.doi.org/10.1016/S0191-2615(03)00026-2.

Rahman, M.M., Wirasinghe, S.C., Kattan, L., 2018. Analysis of bus travel time distributions for varying horizons and real-time applications. Transp. Res. C 86, 453–466. http://dx.doi.org/10.1016/j.trc.2017.11.023.

Song, W., Han, K., Wang, Y., Friesz, T.L., del Castillo, E., 2018. Statistical metamodeling of dynamic network loading. Transp. Res. B 117, 740–756. http://dx.doi.org/10.1016/j.trb.2017.08.018.

Szeto, W.Y., Jiang, Y., 2014. Transit route and frequency design: Bi-level modeling and hybrid artificial bee colony algorithm approach. Transp. Res. B 67, 235–263. http://dx.doi.org/10.1016/j.trb.2014.05.008.

Toledo, T., Cats, O., Burghout, W., Koutsopoulos, H.N., 2010. Mesoscopic simulation for transit operations. Transp. Res. C 18, 896–908. http://dx.doi.org/10.1016/j.trc.2010.02.008.

Wang, Y., Zhang, D., Hu, L., Yang, Y., Lee, L.H., 2017. A data-driven and optimal bus scheduling model with time-dependent traffic and demand. IEEE Trans. Intell. Trans. Syst. 18, 2443–2452. http://dx.doi.org/10.1109/TITS.2016.2644725.

Wolsey, L.A., 1998. Integer Programming. John Wiley & Sons.

Wong, R.C.W., Yuen, T.W.Y., Fung, K.W., Leung, J.M.Y., 2008. Optimizing timetable synchronization for rail mass transit. Transp. Sci. 42, 57–69. http://dx.doi.org/10.1287/trsc.1070.0200.

Wu, W., Liu, R., Jin, W., 2016. Designing robust schedule coordination scheme for transit networks with safety control margins. Transp. Res. B 93, 495–519. http://dx.doi.org/10.1016/j.trb.2016.07.009.

Wu, W., Liu, R., Jin, W., Ma, C., 2019. Stochastic bus schedule coordination considering demand assignment and rerouting of passengers. Transp. Res. B 121, 275–303. http://dx.doi.org/10.1016/j.trb.2019.01.010.

Wu, X., Lu, J., Wu, S., Zhou, X., 2021. Synchronizing time-dependent transportation services: Reformulation and solution algorithm using quadratic assignment problem. Transp. Res. B 152, 140–179.

Xie, J., Wong, S.C., Zhan, S., Lo, S.M., Chen, A., 2020. Train schedule optimization based on schedule-based stochastic passenger assignment. Transp. Res. E 136, 101882. http://dx.doi.org/10.1016/j.tre.2020.101882.

Xie, J., Zhan, S., Wong, S.C., Lo, S.M., 2021. A schedule-based timetable model for congested transit networks. Transp. Res. C.

Ye, H., Liu, R., 2016. A multiphase optimal control method for multi-train control and scheduling on railway lines. Transp. Res. B 93, 377–393. http://dx.doi.org/10.1016/j.trb.2016.08.002.

Yu, B., Lam, W.H.K., Tam, M.L., 2011. Bus arrival time prediction at bus stop with multiple routes. Transp. Res. C 19, 1157–1170. http://dx.doi.org/10.1016/j.trc.2011.01.003.

Yue, Y., Han, J., Wang, S., Liu, X., 2017. Integrated train timetabling and rolling stock scheduling model based on time-dependent demand for urban rail transit. Comput.-Aided Civ. Infrastruct. Eng. 32, 856–873. http://dx.doi.org/10.1111/mice.12300.

Zhao, W., Liu, R., Ngoduy, D., 2018. A bilevel programming model for autonomous intersection control and trajectory planning. Transportmetrica A 1–25. http://dx.doi.org/10.1080/23249935.2018.1563921.

Zhou, Y., Yao, L., Chen, Y., Gong, Y., Lai, J., 2017. Bus arrival time calculation model based on smart card data. Transp. Res. C 74, 81–96. http://dx.doi.org/10.1016/j.trc.2016.11.014.